Bulletin of Mathematical Biology (2020) 82:73
https://doi.org/10.1007/s11538-020-00747-6

Society for Mathematical Biology

ORIGINAL PAPER

Modeling the Effects of Meteorological Factors and Unreported Cases on Seasonal Influenza Outbreaks in Gansu Province, China

Shuang-Lin Jing[1] · **Hai-Feng Huo**[1] · **Hong Xiang**[1]

Received: 13 September 2019 / Accepted: 14 May 2020 / Published online: 12 June 2020

Abstract

Influenza usually breaks out seasonally in temperate regions, especially in winter, infection rates and mortality rates of influenza increase significantly, which means that dry air and cold temperatures accelerate the spread of influenza viruses. However, the meteorological factors that lead to seasonal influenza outbreaks and how these meteorological factors play a decisive role in influenza transmission remain unclear. During the epidemic of infectious diseases, the neglect of unreported cases leads to an underestimation of infection rates and basic reproduction number. In this paper, we propose a new non-autonomous periodic differential equation model with meteorological factors including unreported cases. First, the basic reproduction number is obtained and the global asymptotic stability of the disease-free periodic solution is proved. Furthermore, the existence of periodic solutions and the uniformly persistence of the model are demonstrated. Second, the best-fit parameter values in our model are identified by the MCMC algorithm on the basis of the influenza data in Gansu province, China. We also estimate that the basic reproduction number is 1.2288 (95% CI:(1.2287, 1.2289)). Then, to determine the key parameters of the model, uncertainty and sensitivity analysis are explored. Finally, our results show that influenza is more likely to spread in low temperature, low humidity and low precipitation environments. Temperature is a more important factor than relative humidity and precipitation during the influenza epidemic. In addition, our results also show that there are far more unreported cases than reported cases.

Keywords Influenza · Meteorological factor · Unreported cases · Mathematical model · Parameter estimation

✉ Hai-Feng Huo
hfhuo@lut.edu.cn

[1] Department of Applied Mathematics, Lanzhou University of Technology, Lanzhou 730050, Gansu, People's Republic of China

1 Introduction

Influenza is an acute respiratory infection caused by an influenza virus. Influenza is a highly contagious and rapidly spreading disease that spreads mainly through droplets in the air, human to human contact, and contact between people and contaminated objects. Typical clinical symptoms are systemic fever, generalized weakness, and respiratory infections. Influenza viruses cause widespread morbidity and mortality among human populations worldwide: In China alone, there were 153 deaths and 765,186 infections in 2018 (National Health Commission of the People's Republic of China 2019). In particular, due to the relatively backward medical and health conditions, influenza is particularly serious in Gansu Province, China. In temperate regions like China, the effects of influenza occur mainly in the winter (Lowen et al. 2007; Mourtzoukou and Falagas 2007); that is, influenza outbreaks are highly predictable seasonal patterns. In the northern hemisphere, influenza viruses are prevalent from November to March (Viboud et al. 2006). Influenza is highly contagious and spreads rapidly. This feature is the root cause of the significant morbidity and economic burden of health care.

Several factors are thought to be responsible for the seasonal outbreak of influenza, including temperature, humidity, rainfall, pH, salinity, indoor crowding, and sunlight (Eccles 2002; Kudo et al. 2019; Lowen and Steel 2014; Sooryanarain and Elankumaran 2015; Tamerius et al. 2010). A study that analyzed data from more than 30 years in the USA found that absolute humidity decline (depending on relative humidity and temperature) is closely related to the number of influenza-related deaths (Shaman et al. 2010). The seasonality of the flu depends to a large extent on temperature and humidity. Cool and dry conditions can improve the survival rate and transmission rate of influenza virus in temperate regions (Sooryanarain and Elankumaran 2015).

There are many studies on the effects of meteorological factors such as temperature and humidity on influenza viruses (Foxman et al. 2015; Kudo et al. 2019; Loosli et al. 1943; Lowen and Steel 2014; Lowen et al. 2007; Mäkinen et al. 2009; Pyankov et al. 2018; Tamerius et al. 2013). As early as, Loosli et al. (1943) showed that influenza viruses were more susceptible to inactivation in high humidity atmospheres. Lowen et al. (2007) allowed hundreds of guinea pigs to contact the same human influenza virus at different temperatures and humidity. The team found that at room temperature, the spread of influenza peaked at relatively low humidity (20–35%). Influenza is less likely to spread when the humidity is around 50%, and does not spread at all when the humidity exceeds 80%. The study also found that temperature was a more important factor than humidity. Under certain conditions of humidity, the guinea pigs would get the flu at a temperature of 5 °C, and the flu virus would not invade when the temperature is high. Shaman et al. (2010) showed that the absolute humidity alone was sufficient to produce the seasonality of influenza. This finding provides epidemiological support for the hypothesis that absolute humidity drives seasonal changes in influenza in temperate regions. Mäkinen et al. (2009) showed that low temperature and low humidity were associated with increased respiratory infections. Lowen and Steel (2014) showed that the spread of influenza virus was strongly regulated by temperature and humidity. They revealed a strong correlation between flu incidence in temperate regions and local humidity and temperature conditions. Kudo et al. (2019) found that exposure of mice

to low humidity and low temperatures made them more susceptible to influenza. They showed that dry air combined with cold temperature could achieve viral transmission.

There are relatively few studies on the transmission model of the correlation between influenza and weather factors such as temperature and humidity (Handel et al. 2013; Xing et al. 2017). Handel et al. (2013) showed that the temperature decay rate of influenza virus in the environment was described as $\delta(T) = \alpha e^{\gamma T}$, where T was the temperature, α and γ were constants. Xing et al. (2017) used the temperature dependent decay function of the influenza virus studied by Handel et al. (2013) to evaluate the cause of recurrence of H7N9 avian influenza in China. Other studying the effects of temperature, humidity, or other factors on infectious diseases or other social epidemics; please see Bao and Li (2020), Bao et al. (2020), Guo et al. (2019), Huo et al. (2018, 2019a, b), Ma (2019), Meng and Wu (2018), Tang et al. (2018), Wang et al. (2016a), Xiang et al. (2019), Zhao et al. (2019), Zhang et al. (2019) and references cited therein.

The reported cases usually are only a small fraction of the total number of cases during the outbreak of infectious diseases. Unreported cases are the majority of the total number of cases. Recently, many scholars have studied unreported cases during the outbreak of epidemics (Ducrot et al. 2019; Gamado et al. 2014, 2017; Grubaugh et al. 2019; Magal and Webb 2018). The neglect of unreported cases often leads to an underestimation of infection rates and basic reproduction number in epidemic model (Gamado et al. 2017), which will have a serious impact on the control spread of disease. Gamado et al. (2014) showed that epidemiological and socioeconomic factors were the main causes of underreporting. Magal and Webb (2018) analyzed the relationship between unreported cases and reported cases. They showed that the proportion of unreported cases to reported cases was very high, which was of great significance in implementing measures to control the epidemic. Grubaugh et al. (2019) discovered an unreported outbreak of Zika virus in Cuba through the detection of tourism data and genomics.

Motivated by the above (Handel et al. 2013; Sooryanarain and Elankumaran 2015; Wang et al. 2016b; Xing et al. 2017), we propose a new non-autonomous differential equation model with meteorological factors in this paper. Since the poor public medical conditions in Gansu Province, the reported cases are only a part, and most of the influenza patients are not treated or treated with family therapy, we also introduce unreported compartment in the model. We derive the basic reproduction number and study stability of disease-free periodic solution. We also demonstrate the existence of positive periodic solutions and the uniformly persistence of the model. Further, we identify the best-fit parameter values in our model by the MCMC algorithm on the basis of the influenza data in Gansu province, China. We also estimate that the basic reproduction number is 1.2288 (95% CI:(1.2287, 1.2289)). Then, we explore uncertainty and sensitivity analysis to determine the key parameters of the model.

The organization of this paper is as follows: In Sect. 2, we propose a new non-autonomous differential equation influenza model with meteorological factors, and we get the invariant set of the model and the basic reproduction number R_0. The global asymptotic stability of the disease-free periodic solution of the model is also demonstrated. The uniformly persistence of model and the existence of a positive T-periodic solution have also been proved. In Sect. 3, we use the MCMC algorithm

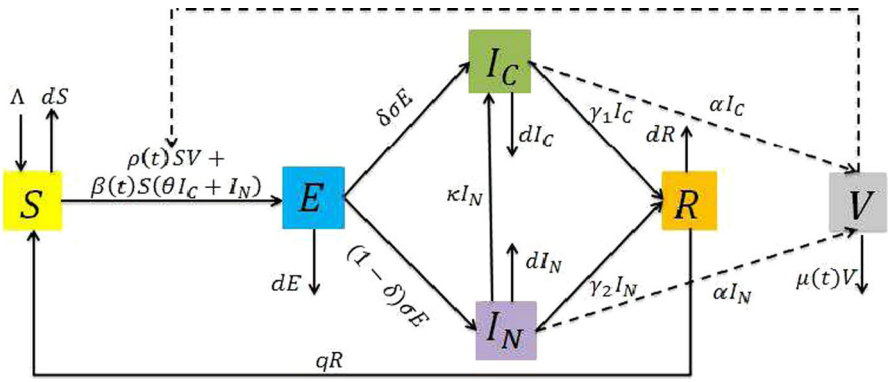

Fig. 1 Flowchart of the influenza model (1) (Color figure online)

to estimate the unknown parameters and initial values of the model. The basic reproduction number R_0 of the model and its confidence interval are solved by numerical methods. In Sect. 4, The effects of several meteorological factors on the number of influenza cases are studied. At the same time, we use the LHS (Latin hypercube sampling) method and the PRCC (partial rank correlation coefficient) method to obtain the uncertainty and sensitivity of the unknown parameters of the model. In Sect. 5, we give some discussions and conclusions.

2 Model Derivation

2.1 System Description

The total population is divided into five compartments: $S(t)$, $E(t)$, $I_N(t)$, $I_C(t)$ and $R(t)$. $S(t)$ represents the number of susceptible individuals; $E(t)$ denotes the number of exposed individuals; $I_N(t)$ represents the unreported cases by the CDC in Gansu Province, including asymptomatic infected individuals and some symptomatic infected individuals; $I_C(t)$ represents the reported cases by the CDC in Gansu Province; $R(t)$ represents the number of refectious individuals. Let $V(t)$ be the density of influenza virus in a polluted environment, including droplets in the air, contaminated items, etc. The total number of population at time t is given by

$$N(t) = S(t) + E(t) + I_N(t) + I_C(t) + R(t).$$

The population flow among those compartments is shown in the following diagram (see Fig. 1).

Human infection can be divided into two categories: One is the transmission rate of direct contact between susceptible individuals and infected individuals, which is expressed in $\beta(t)$; the other is the transmission rate of indirect contact between susceptible individuals and influenza viruses in the environment, which is expressed in $\rho(t)$. As we mentioned in Introduction, the viability of influenza viruses is affected by

Table 1 The parameters description of model (1)

Parameters	Description (units)
Λ	The recruitment rate of the susceptible individuals (month^{-1})
d	The natural mortality rate of the population (month^{-1})
θ	The modification factor in transmission coefficient of the reported infected individuals (none)
δ	The proportion of infected individuals notified by CDC in Gansu Province (none)
$1/\sigma$	The mean incubation period of the infected individuals (month)
q	The progression rate of the recovered individuals (month^{-1})
γ_1	The recovery rate of reported infected individuals (month^{-1})
γ_2	The recovery rate of unreported infected individuals (month^{-1})
α	The virus shedding rate from infected individuals (month^{-1})
κ	The treatment rate of unreported infected individuals (month^{-1})
$\mu(t)$	The clearance rate of influenza virus (month^{-1})
$\beta(t)$	The direct transmission rate between susceptible individuals and infected individuals (none)
$\rho(t)$	The indirect transmission rate between susceptible individuals and infected individuals (none)

meteorological factors. Therefore, the clearance rate of influenza virus is a function of time, which is expressed by $\mu(t)$. All the parameters and periodic functions with period of T are assumed to be positive and detailed definitions are given in Table 1.

We establish a non-autonomous differential equation as

$$\begin{cases} \dfrac{\mathrm{d}S}{\mathrm{d}t} = \Lambda + qR - \beta(t)S(\theta I_C + I_N) - \rho(t)SV - dS, \\ \dfrac{\mathrm{d}E}{\mathrm{d}t} = \beta(t)S(\theta I_C + I_N) + \rho(t)SV - \sigma E - dE, \\ \dfrac{\mathrm{d}I_N}{\mathrm{d}t} = (1-\delta)\sigma E - \gamma_2 I_N - dI_N - \kappa I_N, \\ \dfrac{\mathrm{d}I_C}{\mathrm{d}t} = \delta\sigma E - \gamma_1 I_C - dI_C + \kappa I_N, \\ \dfrac{\mathrm{d}R}{\mathrm{d}t} = \gamma_1 I_C + \gamma_2 I_N - qR - dR, \\ \dfrac{\mathrm{d}V}{\mathrm{d}t} = \alpha(I_C + I_N) - \mu(t)V. \end{cases} \tag{1}$$

2.2 Positively Invariant Set

Lemma 2.2.1 *Define*

$$\Omega = \Big\{(S, E, I_N, I_C, R, V) \in \mathbb{R}^6_+ : 0 \le S, E, I_N, I_C, R, N = S + E + I_N + I_C + R \le \frac{\Lambda}{d}, 0 \le V \le \frac{2\alpha\Lambda}{dU}\Big\}.$$

The trajectories of the model (1) are bounded, and the set Ω is a positive invariant set. In particular, $(S(t), E(t), I_N(t), I_C(t), R(t), V(t))$ is positive for all $t > 0$ if the initial values $S(0) > 0$, $E(0) > 0$, $I_N(0) > 0$, $I_C(0) > 0$, $R(0) > 0$ and $V(0) > 0$ at $t = 0$.

Proof First, we prove the nonnegativity of the solution of model (1). By the continuous dependence of solutions with respect to initial values, we only need to prove that when the initial values $S(0) > 0, E(0) > 0, I_N(0) > 0, I_C(0) > 0, R(0) > 0$ and $V(0) > 0$, $(S(t), E(t), I_N(t), I_C(t), R(t), V(t))$ is positive for all $t > 0$. Let

$$W(t) = \min\left\{S(t), E(t), I_N(t), I_C(t), R(t), V(t)\right\}, \quad \text{for all } t > 0.$$

It is clear that $W(0) > 0$. Assuming that there exists a $t_1 > 0$ such that $W(t_1) = 0$ and $W(t) > 0$, for all $t \in [0, t_1)$.

If $W(t_1) = S(t_1)$, then $I_N(t) \geq 0$, $I_N(t) \geq 0$, $R(t) \geq 0$ and $V(t) \geq 0$ for all $t \in [0, t_1]$. From the first equation of model (1), we can obtain

$$\frac{\mathrm{d}S}{\mathrm{d}t} \geq -\beta(t)S(\theta I_C + I_N) - \rho(t)SV - \mathrm{d}S, \quad \text{for all } t \in [0, t_1].$$

Thus, we have

$$0 = S(t_1) \geq S(0)\mathrm{e}^{-\int_0^{t_1}[\beta(\zeta)(\theta I_C + I_N) + \rho(\zeta)V + d]d\zeta} > 0,$$

which leads to a contradiction. Thus, $S(t) > 0$ for all $t \geq 0$.

Similarly, we can also prove that $E(t) > 0$, $I_N(t) > 0$, $I_N(t) > 0$, $R(t) > 0$ and $V(t) > 0$ for all $t \geq 0$.

Second, we prove that the solution of model (1) is uniformly and ultimately bounded. From model (1), we know that the total population $N(t)$ satisfies the following equation:

$$\frac{\mathrm{d}N}{\mathrm{d}t} = \frac{\mathrm{d}S}{\mathrm{d}t} + \frac{\mathrm{d}E}{\mathrm{d}t} + \frac{\mathrm{d}I_N}{\mathrm{d}t} + \frac{\mathrm{d}I_C}{\mathrm{d}t} + \frac{\mathrm{d}R}{\mathrm{d}t} = \Lambda - dN.$$

This implies

$$N(t) = \frac{\Lambda}{d} + \big(N(0) - \frac{\Lambda}{d}\big)\mathrm{e}^{-dt},$$

where $N(0)$ represents the total population at time $t = 0$.

Then it follows that $\lim_{t\to\infty} \sup N(t) \leq \frac{\Lambda}{d}$.

Through the last equation of model (1), we obtain

$$\frac{\mathrm{d}V}{\mathrm{d}t} = \alpha(I_C + I_N) - \mu(t)V \leq \frac{2\Lambda\alpha}{d} - \mu(t)V.$$

Since $\mu(t)$ is a continuous, positive periodic function, it is easy to get $\mu(t)$ to be bounded. Let us assume that $U = \min\{\mu(t)\}$, for $\forall t \geq 0$. Therefore, we get the following inequality:

$$\frac{\mathrm{d}V}{\mathrm{d}t} = \frac{2\Lambda\alpha}{d} - \mu(t)V \leq \frac{2\Lambda\alpha}{d} - UV$$

This implies

$$V(t) \leq \frac{2\Lambda\alpha}{dU} + \left(V(0) - \frac{2\Lambda\alpha}{dU}\right)\mathrm{e}^{-Ut},$$

where $V(0)$ indicates the number of viruses at time $t = 0$.

Then it follows that $\lim_{t\to\infty} \sup V(t) \leq \frac{2\Lambda\alpha}{dU}$. Therefore, we obtain the positive invariant set of model (1) as

$$\Omega = \Big\{(S, E, I_N, I_C, R, V) \in \mathbb{R}^6_+ : 0 \leq S, E, I_N, I_C, R, N = S + E + I_N + I_C + R \leq \frac{\Lambda}{d}, 0 \leq V \leq \frac{2\alpha\Lambda}{dU}\Big\}. \tag{2}$$

□

2.3 The Basic Reproduction Number for the Periodic System

Taking into account the cyclical changes in the influenza, we can examine the basic reproduction number of the periodic model (1). It is easy to see that model (1) always has a disease-free periodic solution $P_0 = (\frac{\Lambda}{d}, 0, 0, 0, 0, 0)$. Then we can use the theory proposed by Wang and Zhao (2008) to define basic reproduction number of model (1). Let $x = (E, I_N, I_C, R, V, S)^T$, model (1) can be written as

$$\frac{\mathrm{d}x(t)}{\mathrm{d}t} = \mathcal{F}(t, x) - \mathcal{V}(t, x),$$

where

$$\mathcal{F}(t, x) = \begin{bmatrix} \beta(t)S(I_N + \theta I_C) + \rho(t)SV \\ 0 \\ 0 \\ 0 \\ 0 \\ 0 \end{bmatrix},$$

and

$$\mathcal{V}(t,x)=\begin{bmatrix}(\sigma+d)E\\ -(1-\delta)\sigma E+(\gamma_2+d+\kappa)I_N\\ -\delta\sigma E+(\gamma_1+d)I_C-\kappa I_N\\ -\gamma_2 I_N-\gamma_1 I_C+(q+d)R\\ -\alpha(I_N+I_C)+\mu(t)V\\ -\Lambda-qR+\beta(t)S(I_N+\theta I_C)+\rho(t)SV+dS\end{bmatrix}.$$

It is very clear that the conditions (A1)–(A5) of the theory proposed by Wang and Zhao (2008) are satisfied. Let $f(t,x(t))=\mathcal{F}(t,x)-\mathcal{V}(t,x)$, and we define

$$M(t):=\Big(\frac{\partial f_6(t,x^0(t))}{\partial x_6}\Big), \tag{3}$$

where $x^0(t)=(0,0,0,0,0,\frac{\Lambda}{d})$ is the disease-free periodic solution.

Let $\Phi_M(t)$ be the monodromy matrix of the linear T-periodic system $\frac{\mathrm{d}z}{\mathrm{d}t}=M(t)z$. Therefore, we obtain $\Phi_M(t)=\mathrm{e}^{-dt}$, which implies the spectral radius $\rho(\Phi_M(T))$ of $\Phi_M(T)$ is less than unity. It is very clear that the condition (A6) of the theory proposed by Wang and Zhao (2008) is also satisfied.

In order to verify that condition (A7) is established, we define $F(t)=\Big(\frac{\partial\mathcal{F}_i(t,x^0(t))}{\partial x_j}\Big)_{1\le i,j\le 5}$ and $V(t)=\Big(\frac{\partial\mathcal{V}_i(t,x^0(t))}{\partial x_j}\Big)_{1\le i,j\le 5}$, where $\mathcal{F}_i(t,x)$ and $\mathcal{V}_i(t,x)$ are the i-th component of $\mathcal{F}(t,x)$ and $\mathcal{V}(t,x)$, respectively. Then, we obtain

$$F(t)=\begin{bmatrix}0&\frac{\beta(t)\Lambda}{d}&\frac{\beta(t)\Lambda\theta}{d}&0&\frac{\rho(t)\Lambda}{d}\\ 0&0&0&0&0\\ 0&0&0&0&0\\ 0&0&0&0&0\\ 0&0&0&0&0\end{bmatrix}, \tag{4}$$

and

$$V(t)=\begin{bmatrix}\sigma+d&0&0&0&0\\ -(1-\delta)\sigma&\gamma_2+d+\kappa&0&0&0\\ -\delta\sigma&-\kappa&\gamma_1+d&0&0\\ 0&-\gamma_2&-\gamma_1&q+d&0\\ 0&-\alpha&-\alpha&0&\mu(t)\end{bmatrix}. \tag{5}$$

It is very clear that $F(t)$ is nonnegative and $-V(t)$ is cooperative in the sense that the off-diagonal elements of $-V(t)$ are nonnegative.

Let $Y(t,s)$, $t\ge s$, be the evolution operator of the linear T-periodic system

$$\frac{\mathrm{d}y}{\mathrm{d}t}=-V(t)y. \tag{6}$$

That is, for each $s \in \mathbb{R}$, the 5×5 matrix $Y(t, s)$ satisfies

$$\frac{\mathrm{d}Y(t,s)}{\mathrm{d}t} = -V(t)Y(t,s), \quad \forall t \geq s, \quad Y(s,s) = I, \tag{7}$$

where I is the 5×5 identity matrix.

Let $\Phi_{-V}(t)$ be the monodromy matrix of the linear T-periodic system $\frac{\mathrm{d}y}{\mathrm{d}t} = -V(t)y$, and it is clear that

$$\rho(\Phi_{-V}(T)) = \max\left\{\mathrm{e}^{-(\sigma+d)T}, \mathrm{e}^{-(\gamma_2+d+\kappa)T}, \mathrm{e}^{-(\gamma_1+d)T}, \mathrm{e}^{-(q+d)T}, \mathrm{e}^{-\mu(T)T}\right\} < 1.$$

Therefore, the condition (A7) of the theory proposed by Wang and Zhao (2008) is also satisfied.

According to the method in Wang and Zhao (2008), we assume that $\phi(s)$ is the initial distribution of infectious individuals, and $\phi(s)$ is T-periodic in s. Therefore, $F(s)\phi(s)$ is the distribution of new individuals generated by infected individuals at time s. $Y(t, s)F(s)\phi(s)$ gives the distribution of infected individuals who are newly infected by $\phi(s)$ and remain in the infected compartment at time s, when $t \geq s$. Then we define

$$\psi(t) := \int_{-\infty}^{t} Y(t,s)F(s)\phi(s)\mathrm{d}s = \int_{0}^{\infty} Y(t,t-a)F(t-a)\phi(t-a)\mathrm{d}a, \tag{8}$$

where $\psi(t)$ represents the distribution of accumulated newly infected individuals produced by all infected individuals $\phi(s)$ introduced at previous time to t.

Let C_T be the ordered Banach space of all T-periodic functions from $\mathbb{R}$ to $\mathbb{R}^5$ with the maximum norm $\|\cdot\|$ and the positive cone $C_T^+ := \{\phi \in C_T : \phi(t) \geq 0, \ \forall t \in \mathbb{R}\}$. According to the method in Wang and Zhao (2008), we can define a linear operator $L : C_T \to C_T$ as follows

$$(L\phi)(t) = \int_{0}^{\infty} Y(t,t-a)F(t-a)\phi(t-a)\mathrm{d}a, \ \forall t \in \mathbb{R}, \ \phi \in C_T. \tag{9}$$

L is called the next-generation infection operator and the spectral radius of L is defined as the basic reproduction number R_0. Therefore, the basic reproduction number R_0 of model (1) can be expressed as follows

$$R_0 := \rho(L). \tag{10}$$

Lemma 2.3.1 [see Theorem 2.2 in Wang and Zhao (2008)]. *The following statements are valid:*

(1) $R_0 = 1$ *if and only if* $\rho(\Phi_{F-V}(T)) = 1$.
(2) $R_0 > 1$ *if and only if* $\rho(\Phi_{F-V}(T)) > 1$.
(3) $R_0 < 1$ *if and only if* $\rho(\Phi_{F-V}(T)) < 1$.

Therefore, the disease-free periodic solution ρ_0 *of model* (1) *is locally asymptotically stable if* $R_0 < 1$ *and unstable if* $R_0 > 1$.

In order to calculate the basic reproduction number R_0 of model (1), according to Theorem 2.1 in Wang and Zhao (2008), we introduce the linear T-periodic system as follows

$$\frac{\mathrm{d}\omega}{\mathrm{d}t} = \Big[-V(t) + \frac{F(t)}{\lambda}\Big]\omega,\ t \in \mathbb{R}, \tag{11}$$

where parameter $\lambda \in (0, \infty)$. Then, let the evolution operator of system (11) on $\mathbb{R}^5$ be $W(t, s, \lambda),\ t \geq s,\ s \in \mathbb{R}$. It is clear that $\Phi_{F-V}(t) = W(t, 0, 1),\ t \geq 0$ can be obtained. Hence, we derive

$$\Phi_{F/\lambda - V}(t) = W(t, 0, \lambda),\ t \geq 0,$$

where

$$-V(t) + \frac{F(t)}{\lambda} = \begin{bmatrix} -(\sigma + d) & \frac{\beta(t)\Lambda}{\lambda d} & \frac{\beta(t)\Lambda\theta}{\lambda d} & 0 & \frac{\rho(t)\Lambda}{\lambda d} \\ (1-\delta)\sigma & -(\gamma_2 + d + \kappa) & 0 & 0 & 0 \\ \delta\sigma & \kappa & -(\gamma_1 + d) & 0 & 0 \\ 0 & \gamma_2 & \gamma_1 & -(q+d) & 0 \\ 0 & \alpha & \alpha & 0 & -\mu(t) \end{bmatrix}.$$

Lemma 2.3.2 [see Theorem 2.1 in Wang and Zhao (2008)]. *The following statements are valid:*

(1) *If* $\rho(W(T, 0, \lambda)) = 1$ *has a positive solution* λ_0*, then* λ_0 *is an eigenvalue of* L*, and hence* $R_0 > 0$.
(2) *If* $R_0 > 0$*, then* $\lambda = R_0$ *is the unique solution of* $\rho(W(T, 0, \lambda)) = 1$.
(3) $R_0 = 0$ *if and only if* $\rho(W(T, 0, \lambda)) < 1$ *for all* $\lambda > 0$.

Therefore, we can use the numerical algorithm to calculate the basic reproduction number according to (2) in Lemma 2.3.2.

2.4 Extinction of the Disease

Let $(\mathbb{R}^n, \mathbb{R}^n_+)$ be the standard n-dimensional Euclidean space. For $u, v \in \mathbb{R}^n$, if $u - v \in \mathbb{R}^n_+$, then $u \geq v$; if $u - v \in \mathbb{R}^n_+ \backslash \{0\}$, then $u > v$; if $u - v \in Int(\mathbb{R}^n_+)$, then $u \gg v$.

Let $A(t)$ be a continuous, cooperative and irreducible $n \times n$ matrix function of the T-period, and $\Phi_A(t)$ is the fundamental solution matrix of the following system

$$\frac{\mathrm{d}x(t)}{\mathrm{d}t} = A(t)x(t).$$

Let $\rho(\Phi_A(T))$ be the spectral radius of $\Phi_A(T)$. Thus each element of matrix $\Phi_A(T)$ is positive at $T > 0$ (Aronsson and Kellogg 1978; Hirsch 1985). Through Perron-Frobenius theorem (Smith and Waltman 1995), $\rho(\Phi_A(T))$ is the principal eigenvalue of $\Phi_A(T)$ in the sense that it is simple and admits an eigenvector $v^* \gg 0$. Therefore, we have a conclusion as follows

Lemma 2.4.1 [see Zhang and Zhao (2007)]. *Let* $p = \frac{1}{T}\ln\rho(\Phi_A(T))$. *Then there exists a positive,* T*-periodic function* $v(t)$ *such that* $e^{pt}v(t)$ *is a solution of* $\frac{\mathrm{d}x(t)}{\mathrm{d}t} = A(t)x(t)$.

Theorem 2.4.1 *Disease-free periodic solution* $P_0 = (\frac{\Lambda}{d}, 0, 0, 0, 0, 0)$ *of the model* (1) *is globally asymptotically stable if* $R_0 < 1$ *in* Ω.

Proof By Lemma 2.3.1, we obtain that the disease-free periodic solution $P_0 = (\frac{\Lambda}{d}, 0, 0, 0, 0, 0)$ is locally asymptotically stable for $R_0 < 1$, and the disease-free periodic solution $P_0 = (\frac{\Lambda}{d}, 0, 0, 0, 0, 0)$ is unstable for $R_0 > 1$. Therefore, we only need to prove that the disease-free periodic solution $P_0 = (\frac{\Lambda}{d}, 0, 0, 0, 0, 0)$ is globally attractive for $R_0 < 1$.

From model (1) and lemma (2.2.1), we have

$$\frac{\mathrm{d}(S(t)+E(t)+I_N(t)+I_C(t)+R(t))}{\mathrm{d}t} = \Lambda - d(S(t)+E(t)+I_N(t)+I_C(t)+R(t)),$$

which implies that

$$\lim_{t\to\infty}\sup(S(t)+E(t)+I_N(t)+I_C(t)+R(t)) \le \frac{\Lambda}{d}.$$

Because $E(t) \ge 0$, $I_N(t) \ge 0$, $I_C(t) \ge 0$ and $R(t) \ge 0$ for all $t \ge 0$, it follows that

$$\lim_{t\to\infty}\sup S(t) \le \frac{\Lambda}{d}.$$

Thus, for $\forall\eta > 0$, there exists $\bar{t} > 0$ such that $S(t) \le \frac{\Lambda}{d} + \eta$ for $t > \bar{t}$. We consider the following comparison system

$$\begin{cases} \dfrac{\mathrm{d}\hat{E}}{\mathrm{d}t} = \beta(t)(\dfrac{\Lambda}{d}+\eta)(\theta\hat{I_C}+\hat{I_N}) + \rho(t)(\dfrac{\Lambda}{d}+\eta)\hat{V} - \sigma\hat{E} - d\hat{E}, \\ \dfrac{\mathrm{d}\hat{I_N}}{\mathrm{d}t} = (1-\delta)\sigma\hat{E} - \gamma_2\hat{I_N} - d\hat{I_N} - \kappa\hat{I_N}, \\ \dfrac{\mathrm{d}\hat{I_C}}{\mathrm{d}t} = \delta\sigma\hat{E} - \gamma_1\hat{I_C} - d\hat{I_C} + \kappa\hat{I_N}, \\ \dfrac{\mathrm{d}\hat{R}}{\mathrm{d}t} = \gamma_1\hat{I_C} + \gamma_2\hat{I_N} - q\hat{R} - d\hat{R}, \\ \dfrac{\mathrm{d}\hat{V}}{\mathrm{d}t} = \alpha(\hat{I_C}+\hat{I_N}) - \mu(t)\hat{V}. \end{cases} \tag{12}$$

Let $x = (\hat{E}, \hat{I_N}, \hat{I_C}, \hat{R}, \hat{V})^{\mathrm{T}}$, system (12) is equivalent to the following equation

$$x' = \big(F(t) - V(t) + \eta m(t)\big)x,$$

where

$$m(t) = \begin{bmatrix} 0 & \beta(t) & \beta(t)\theta & 0 & \rho(t) \\ 0 & 0 & 0 & 0 & 0 \\ 0 & 0 & 0 & 0 & 0 \\ 0 & 0 & 0 & 0 & 0 \\ 0 & 0 & 0 & 0 & 0 \end{bmatrix}.$$

According to Lemma 2.4.1, we know that there is a positive T-periodic function $v(t)$ such that $e^{pt}v(t)$ is a solution of system (12), where $v(t) = (v_1(t), v_2(t), v_3(t), v_4(t), v_5(t))$ and $p = \frac{1}{T}\ln\rho(\Phi_{F-V+\eta m}(T))$. Next, we choose $\tilde{t} > \bar{t}$ and all small $\tau > 0$ to make the inequality as follows

$$\hat{E}(\tilde{t}) \le \tau v_1(0),\ \hat{I_N}(\tilde{t}) \le \tau v_2(0),\ \hat{I_C}(\tilde{t}) \le \tau v_3(0),\ \hat{R}(\tilde{t}) \le \tau v_4(0),\ \hat{V}(\tilde{t}) \le \tau v_5(0),$$

then, we get

$$\begin{aligned} &\hat{E}(t) \le \tau e^{p(t-\tilde{t})}v_1(t-\tilde{t}),\ \hat{I_N}(t) \le \tau e^{p(t-\tilde{t})}v_2(t-\tilde{t}),\ \hat{I_C}(t) \le \tau e^{p(t-\tilde{t})}v_3(t-\tilde{t}), \\ &\hat{R}(t) \le \tau e^{p(t-\tilde{t})}v_4(t-\tilde{t}),\ \hat{V}(t) \le \tau e^{p(t-\tilde{t})}v_5(t-\tilde{t}),\ t \ge \tilde{t}. \end{aligned}$$

According to the standard comparison principle, we obtain the inequality as follows

$$\begin{aligned} &E(t) \le \hat{E}(t) \le \tau e^{p(t-\tilde{t})}v_1(t-\tilde{t}),\ I_N(t) \le \hat{I_N}(t) \le \tau e^{p(t-\tilde{t})}v_2(t-\tilde{t}), \\ &I_C(t) \le \hat{I_C}(t) \le \tau e^{p(t-\tilde{t})}v_3(t-\tilde{t}),\ R(t) \le \hat{R}(t) \le \tau e^{p(t-\tilde{t})}v_4(t-\tilde{t}), \\ &V(t) \le \hat{V}(t) \le \tau e^{p(t-\tilde{t})}v_5(t-\tilde{t}),\ t \ge \tilde{t}. \end{aligned}$$

From Lemma 2.3.1, we know that if $R_0 < 1$ if and only if $\rho(\Phi_{F-V}(T)) < 1$. Since $\rho(\Phi_{F-V+\eta m}(T))$ is continuous for all small η, we can choose all small $\eta > 0$ such that $\rho(\Phi_{F-V+\eta m}(T)) < 1$. Therefore, we obtain $p < 0$. This means that the following limits are true.

$$\lim_{t\to\infty} E(t) = 0,\ \lim_{t\to\infty} I_N(t) = 0,\ \lim_{t\to\infty} I_C(t) = 0,\ \lim_{t\to\infty} R(t) = 0,\ \lim_{t\to\infty} V(t) = 0.$$

For the first equation of model (1), it is easy to prove that $\lim_{t\to\infty} S(t) = \frac{\Lambda}{d}$ holds. Therefore, the disease-free periodic solution $P_0 = (\frac{\Lambda}{d}, 0, 0, 0, 0, 0)$ of model (1) is globally asymptotically stable.

A numerical simulation of the global asymptotic stability of the disease-free periodic solution P_0 of model (1) is given in "Appendix A," as shown in Fig. 14. □

2.5 Uniform Persistence of the Disease

In this section, we demonstrate the uniform persistence of model (1) by using uniform persistence theory of the periodic epidemic model in Zhao (2017). First, we give the following symbols:

Let X be a metric space, $f : X \to X$ be a continuous map, and $X_0 \subset X$ be an open set. Define

$$\partial X_0 := X \backslash X_0, \quad M_\partial := \Big\{ x \in \partial X_0 : f^n(x) \in \partial X_0, n \geq 0 \Big\}.$$

Assume that A_∂ is a maximal compact invariant set of f in ∂X_0, that is, A_∂ is compact, invariant, possibly empty, and contains every compact invariant subset of ∂X_0. Then a finite sequence $M_1, \ldots, M_k$ of disjoint, compact, and invariant subsets of ∂X_0, each of which is isolated in ∂X_0.

Lemma 2.5.1 [see Theorem 1.3.1 in Zhao (2017)] *Assume that*

(C1) $f(X_0) \subset X_0$ *and* f *has a global attractor* A*;*
(C2) *The maximal compact invariant set* $A_\partial = A \cap M_\partial$ *of* f *in* ∂X_0*, possibly empty, admits a Morse decomposition* $M_1, \ldots, M_k$ *with the following properties:*

(a) M_i *is isolated in* X.
(b) $W^s(M_i) \cap X_0 = \emptyset$ *for each* $1 \leq i \leq k$.

Then there exists $\delta > 0$ *such that for any compact internally chain transitive set* L *with* $L \not\subset M_i$ *for all* $1 \leq i \leq k$*, we have* $\inf_{x \in L} d(x, \partial X_0) > \delta$*, that is to say* $f : X \to X$ *is uniformly persistent with respect to* $(X_0, \partial X_0)$.

Theorem 2.5.1 *If* $R_0 > 1$*, then there is at least one positive periodic solution for model* (1)*, and there is a positive constant* $\varepsilon > 0$ *such that the solution* $(S(t), E(t), I_N(t), I_C(t), R(t), V(t))$ *with initial value condition* $(S(0), E(0), I_N(0), I_C(0), R(0), V(0)) \in \mathbb{R}_+ \times Int(\mathbb{R}^5_+)$ *for each of model* (1) *satisfies*

$$\lim_{t \to \infty} \inf (E(t), I_N(t), I_C(t), R(t), V(t)) \geq (\varepsilon, \varepsilon, \varepsilon, \varepsilon, \varepsilon).$$

Proof Define $X = \{(S, E, I_N, I_C, R, V) \in \mathbb{R}^6_+\}$, $X_0 = \{(S, E, I_N, I_C, R, V) \in \mathbb{R}_+ \times Int(\mathbb{R}^5_+)\}$, and $\partial X_0 = X \backslash X_0$. Let $u(t, x_0)$ be the unique solution of model (1) with an initial value of $x_0 := (S_0, E_0, I_{N0}, I_{C0}, R_0, V_0)$. Let $f : X \to X$ be the Poincaré map associated with model (1); that is,

$$f(x_0) = u(T, x_0), \quad \forall x_0 \in X, \tag{13}$$

where T represents the period, and $u(T, x_0)$ is the only solution of model (1) that satisfies $u(0, x_0) = x_0$.

Obviously, by Lemma 2.2.1, we know that the solution of model (1) is uniformly bounded, which means that f is the point dissipative on X. And, $f : X \to X$ is compact. From the conclusion of Theorem 1.1.3 in Zhao (2017), we can see that f has a global attractor A.

Below we let

$$M_\partial = \Big\{ (S_0, E_0, I_{N0}, I_{C0}, R_0, V_0) \in \partial X_0 : \ f^n(S_0, E_0, I_{N0}, I_{C0}, R_0, V_0) \in \partial X_0, \ \ \forall n \geq 0 \Big\}.$$

Next, we prove that $M_\partial = \{(S, 0, 0, 0, 0, 0) : S \geq 0\}$ holds. Obviously, we can get $(S, 0, 0, 0, 0, 0) \in M_\partial$ for $S \geq 0$. Assume that at least one of E, I_N, I_C, R and V is positive for the initial value $(S, E, I_N, I_C, R, V) = M_\partial$. Then the following inequality is established.

$$
\begin{aligned}
E(t) &= \mathrm{e}^{-(\sigma+d)t}\Big[E_0 + \int_0^t S(\tau)\big(\beta(\tau)(\theta I_C(\tau) + I_N(\tau)) + \rho(\tau)V(\tau)\big)\mathrm{e}^{(\sigma+d)\tau}\mathrm{d}\tau\Big] > 0, \forall t \geq 0,\\
I_N(t) &= \mathrm{e}^{-(\gamma_2+d+\kappa)t}\Big[I_{N0} + \int_0^t (1-\delta)\sigma E(\tau)\mathrm{e}^{(\gamma_2+d+\kappa)\tau}\mathrm{d}\tau\Big] > 0, \forall t \geq 0,\\
I_C(t) &= \mathrm{e}^{-(\gamma_1+d)t}\Big[I_{C0} + \int_0^t \big(\delta\sigma E(\tau) + \kappa I_N(\tau)\big)\mathrm{e}^{(\gamma_1+d)\tau}\mathrm{d}\tau\Big] > 0, \forall t \geq 0,\\
R(t) &= \mathrm{e}^{-(q+d)t}\Big[R_0 + \int_0^t \big(\gamma_1 I_C(\tau) + \gamma_2 I_N(\tau)\big)\mathrm{e}^{(q+d)\tau}\mathrm{d}\tau\Big] > 0, \forall t \geq 0,\\
V(t) &\geq \mathrm{e}^{-Ut}\Big[V_0 + \int_0^t \alpha\big(I_C(\tau) + I_N(\tau)\big)\mathrm{e}^{U\tau}\mathrm{d}\tau\Big] > 0, \forall t \geq 0,
\end{aligned}
$$

where $U = \min\big\{\mu(t), \forall t \geq 0\big\}$. Therefore, there is $(S(t), E(t), I_N(t), I_C(t), R(t), V(t)) \notin \partial X_0$ for a sufficiently small $t > 0$, we get $(S(t), E(t), I_N(t), I_C(t), R(t), V(t)) \notin M_\partial$. This means that $(S_0, E_0, I_{N0}, I_{C0}, R_0, V_0) \notin \partial X_0$, $(S_0, E_0, I_{N0}, I_{C0}, R_0, V_0) \notin M_\partial$. Consequently, we can get $M_\partial = \{(S, 0, 0, 0, 0, 0) : S \geq 0\}$ by the above proof.

By Theorem 2.4.1, we know that $P_0 = (\frac{A}{d}, 0, 0, 0, 0, 0)$ is globally asymptotically stable in set M_∂. Therefore, $A_\partial = \{(\frac{A}{d}, 0, 0, 0, 0, 0)\}$ is the maximal compact invariant set of f in ∂X_0. It is obvious that A_∂ can be acyclic and isolated in set ∂X_0.

In the following, we prove that $W^s(A_\partial) \cap X_0 = \emptyset$ and A_∂ is isolated in set X. For convenience, we denote $x_0 = (S_0, E_0, I_{N0}, I_{C0}, R_0, V_0) \in X_0$. It is known from the continuous dependence of solutions with respect to initial values that there exists $\varrho > 0$ such that for all $(S_0, E_0, I_{N0}, I_{C0}, R_0, V_0) \in X_0$ with $\|x_0 - P_0\| \leq \varrho$. Further, we have

$$\|u(t, x_0) - u(t, P_0)\| \leq \varepsilon, \quad \forall \varepsilon > 0, \quad \forall t \in [0, T].$$

We now claim that

$$\limsup_{n\to\infty} d(f^n(x_0), P_0) \geq \varrho,$$

where $d(x, y)$ represents the distance between x and y. Using the counter-evidence method, we assume that the following formula holds.

$$\limsup_{n\to\infty} d(f^n(x_0), P_0) < \varrho, \text{ for some } x_0 \in X_0.$$

Without loss of generality, we assume that $d(f^n(x_0), P_0) < \varrho$ for any $n > 0$. By the continuous dependence of solutions with respect to initial values, it is known that

$d(u(t, f^n(x_0)), u(t, P_0)) < \varepsilon$ for any $t \in [0, T]$. By continuous and calculation by steps, we obtain

$$d(u(t, x_0), u(t, P_0)) = d(u(t^{'}, f^n(x_0)), u(t^{'}, P_0)) < \varepsilon, \ \forall t \geq 0,$$

where $t = t^{'} + NT, t^{'} \in [0, T]$ and $N = [\frac{t}{T}]$. Thus, this means that there exists $T^{'} > 0$ such that $\frac{\Lambda}{d} - \varepsilon \leq S(t) \leq \frac{\Lambda}{d} + \varepsilon$, $0 \leq E(t) \leq \varepsilon$, $0 \leq I_N(t) \leq \varepsilon$, $0 \leq I_C(t) \leq \varepsilon$, $0 \leq R(t) \leq \varepsilon$ and $0 \leq V(t) \leq \varepsilon$ for $t > T^{'}$. And, we also obtain

$$\frac{\mathrm{d}E}{\mathrm{d}t} \geq \beta(t)\left(\frac{\Lambda}{d} - \varepsilon\right)(\theta I_C + I_N) + \rho(t)\left(\frac{\Lambda}{d} - \varepsilon\right)V - \sigma E - dE.$$

The following comparison system is considered.

$$\begin{cases} \dfrac{\mathrm{d}\tilde{E}}{\mathrm{d}t} = \beta(t)\left(\dfrac{\Lambda}{d} - \varepsilon\right)(\theta \tilde{I_C} + \tilde{I_N}) + \rho(t)\left(\dfrac{\Lambda}{d} - \varepsilon\right)\tilde{V} - \sigma\tilde{E} - d\tilde{E}, \\ \dfrac{\mathrm{d}\tilde{I_N}}{\mathrm{d}t} = (1-\delta)\sigma\tilde{E} - \gamma_2\tilde{I_N} - d\tilde{I_N} - \kappa\tilde{I_N}, \\ \dfrac{\mathrm{d}\tilde{I_C}}{\mathrm{d}t} = \delta\sigma\tilde{E} - \gamma_1\tilde{I_C} - d\tilde{I_C} + \kappa\tilde{I_N}, \\ \dfrac{\mathrm{d}\tilde{R}}{\mathrm{d}t} = \gamma_1\tilde{I_C} + \gamma_2\tilde{I_N} - q\tilde{R} - d\tilde{R}, \\ \dfrac{\mathrm{d}\tilde{V}}{\mathrm{d}t} = \alpha(\tilde{I_C} + \tilde{I_N}) - \mu(t)\tilde{V}. \end{cases} \tag{14}$$

We can represent system (14) as follows

$$x^{'} = \big(F(t) - V(t) - \varepsilon m(t)\big)x,$$

where $x = (\tilde{E}, \tilde{I_N}, \tilde{I_C}, \tilde{R}, \tilde{V})^{\mathrm{T}}$ and

$$m(t) = \begin{bmatrix} 0 & \beta(t) & \beta(t)\theta & 0 & \rho(t) \\ 0 & 0 & 0 & 0 & 0 \\ 0 & 0 & 0 & 0 & 0 \\ 0 & 0 & 0 & 0 & 0 \\ 0 & 0 & 0 & 0 & 0 \end{bmatrix}.$$

According to Lemma 2.4.1, we know that there is a positive T-periodic function $v^*(t)$ such that $e^{p^*t}v^*(t)$ is a solution of system (14), where $v^*(t) = (v_1^*(t), v_2^*(t), v_3^*(t), v_4^*(t), v_5^*(t))$ and $p^* = \frac{1}{T}\ln\rho(\Phi_{F-V-\varepsilon m}(T))$. Note that $\rho(\Phi_{F-V-\varepsilon m}(T)) > 1$. Therefore, according to the comparison principle, we obtain $\lim_{t\to\infty}(E(t), I_N(t), I_C(t), R(t), V(t)) = (\infty, \infty, \infty, \infty, \infty)$, which is contradictory to $0 \leq E(t) \leq \varepsilon$, $0 \leq I_N(t) \leq \varepsilon$, $0 \leq I_C(t) \leq \varepsilon$, $0 \leq R(t) \leq \varepsilon$ and $0 \leq V(t) \leq \varepsilon$. Therefore, $W^s(A_\vartheta) \cap X_0 = \emptyset$ is proved, and A_ϑ is isolated in X. By

Lemma 2.5.1, f is uniformly persistent with respect to $(X_0, \partial X_0)$. Thus, the solution of model (1) is uniformly persistent.

Next, we prove the existence of a positive T-period solution of model (1), that is, f has a fixed point. We consider $(S^*(0), E^*(0), I_N^*(0), I_C^*(0), R^*(0), V^*(0)) \in X_0$, it is easy to see that $S^*(0) \geq 0$, $E^*(0) > 0$, $I_N^*(0) > 0$, $I_C^*(0) > 0$, $R^*(0) > 0$ and $V^*(0) > 0$. We now prove that $S^*(0) > 0$. Using the counter-evidence method, assuming $S^*(0) = 0$, the first equation of model (1) is expressed as follows

$$\frac{\mathrm{d}S^*(t)}{\mathrm{d}t} \geq \Lambda - (\beta(t)(\theta I_C + I_N) + \rho(t)V + d)S = \Lambda - (a(t) + d)S,$$

where $a(t) = \beta(t)(\theta I_C + I_N) + \rho(t)V$. We can get

$$\begin{aligned} S^*(t) &\geq \mathrm{e}^{\int_0^t -(d+a(\tau_1))\mathrm{d}\tau_1} \left[S^*(0) + \int_0^t \Lambda \mathrm{e}^{\int_0^{\tau_2} (d+a(\tau_1))\mathrm{d}\tau_1} \mathrm{d}\tau_2 \right] \\ &= \mathrm{e}^{\int_0^t -(d+a(\tau_1))\mathrm{d}\tau_1} \int_0^t \Lambda \mathrm{e}^{\int_0^{\tau_2} (d+a(\tau_1))\mathrm{d}\tau_1} \mathrm{d}\tau_2, \quad \forall t \geq 0. \end{aligned}$$

Therefore, the following inequality can be obtained.

$$S^*(nT) \geq \mathrm{e}^{\int_0^{nT} -(d+a(\tau_1))\mathrm{d}\tau_1} \int_0^{nT} \Lambda \mathrm{e}^{\int_0^{\tau_2} (d+a(\tau_1))\mathrm{d}\tau_1} \mathrm{d}\tau_2 > 0.$$

From the periodicity of $S^*(t)$, we know that $S^*(0) = S^*(nT) = 0$, $n = 1, 2, 3 \ldots$, which is inconsistent with $S^*(nT) > 0$. Thus, we obtain $S^*(0) > 0$.

From the above proof, we obtain that $u(t, (S^*(0), E^*(0), I_N^*(0), I_C^*(0), R^*(0), V^*(0))) \in Int(\mathbb{R}_+^6)$, and $(S^*(t), E^*(t), I_N^*(t), I_C^*(t), R^*(t), V^*(t))$ is the positive T-period solution of model (1).

A numerical simulation of the positive T-period solution for model (1) is given in "Appendix A," as shown in Fig. 15. □

3 A Case Study

In this section, we estimate the unknown parameters of model (1) on the basis of the influenza data in Gansu Province of China from January 2012 to May 2019 by using MCMC algorithm. By estimating the unknown parameters, we estimate the mean and confidence interval of the basic reproduction number R_0. In addition, we also estimate unreported cases.

3.1 Data Sources

The influenza case data come from the Gansu Provincial Center for Disease Control and Prevention (2019), which is a public health agency in Gansu Province. The data include the number of influenza treated monthly between January 2012 and May 2019,

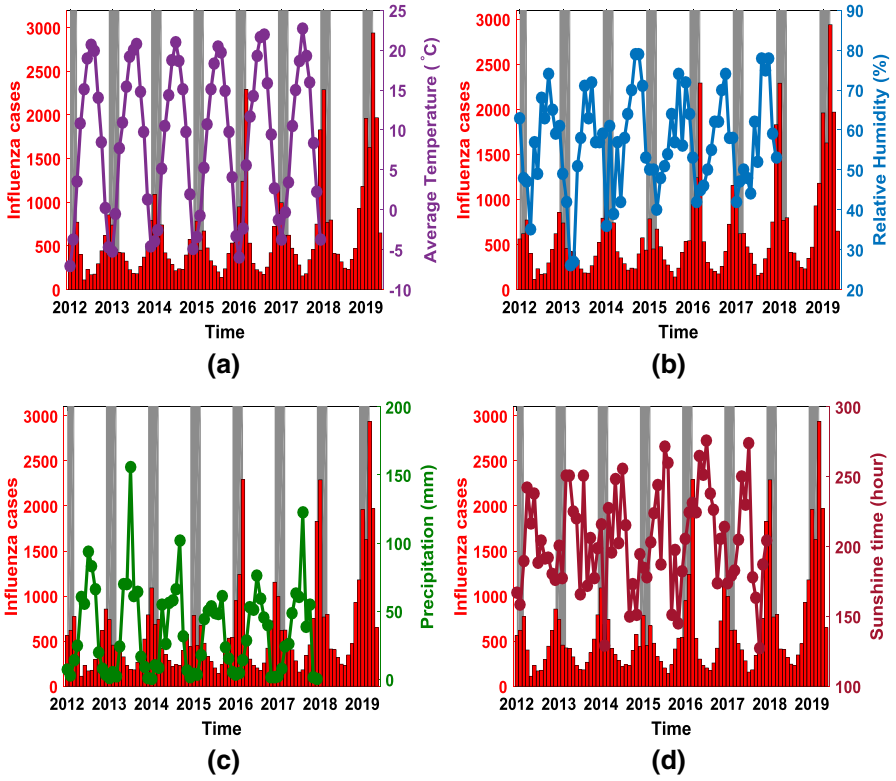

Fig. 2 The number of influenza cases and meteorological factors data. The red histogram indicates the number of influenza cases in Gansu Province from January 2012 to May 2019. The gray area indicates December, January, and February each year. **a** The purple line indicates the monthly average temperature in Gansu Province from January 2012 to December 2018; **b** The blue line indicates the monthly average relative humidity in Gaolan County, Gansu Province, from January 2012 to December 2018; **c** The green line indicates the monthly total precipitation in Gansu Province from January 2012 to December 2018; **d** The deep red line indicates the monthly total sunshine time in Gansu Province from January 2012 to December 2018 (For an explanation of the reference to color in this illustration,the reader is referred to the Web version of this article) (Color figure online)

as indicated by the red histogram in Fig. 2. It can be seen from Fig. 2 that December, January and February are the high incidence of influenza.

The monthly average temperature (MAT), monthly total precipitation (MTP), and monthly total sunshine time (MTST) can be obtained from the Gansu Provincial Bureau of Statistics (2019), as shown in Fig. 2a, c and d. From the National Bureau of Statistics of China (2019b), we can obtain the monthly average relative humidity (MARH) in Gaolan County, Gansu Province , as shown in Fig. 2b.

3.2 Data Analysis and Fitting

In order to study the correlation between several sets of data, we can use the Spearman correlation coefficient to study the correlation between several sets of data from

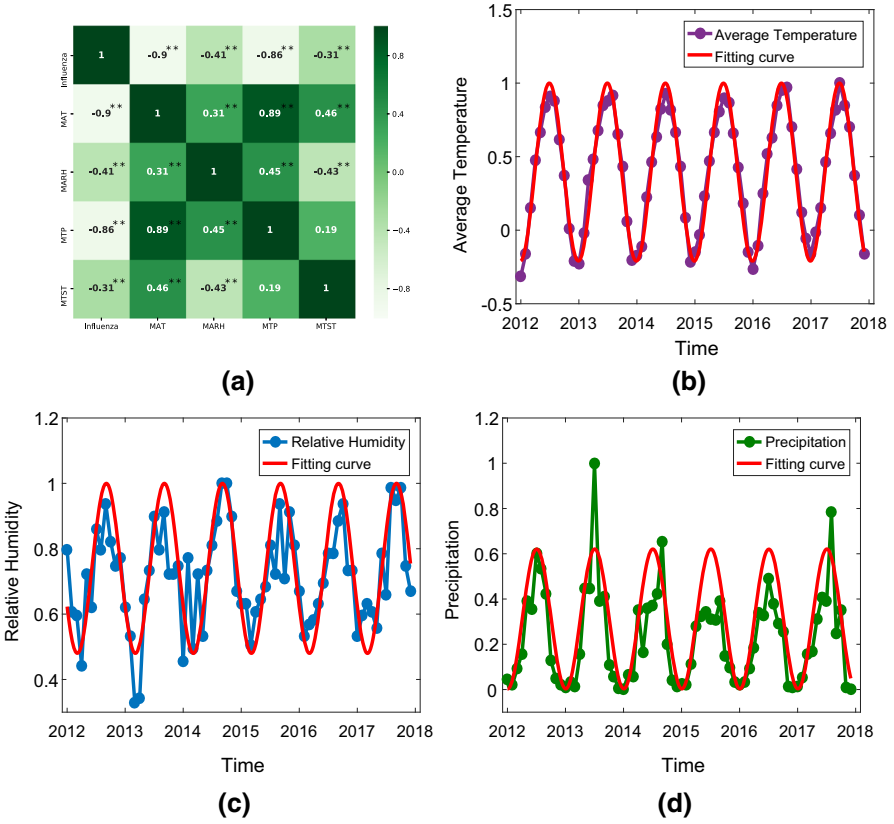

Fig. 3 **a** Significance of correlation coefficient different from zero: $**$ represents $p < 0.01$, $*$ represents $p < 0.05$; **b** The fitting plot of monthly average temperature; **c** The fitting plot of monthly average relative humidity; **d** The fitting plot of monthly total precipitation. The red curve represents the fitting value (For an explanation of the reference to color in this illustration, the reader is referred to the Web version of this article) (Color figure online)

January 2012 to December 2018. We use Python software to calculate the correlation between the four sets of data, as shown in Fig. 3a. The conclusion reveals a significant correlation between influenza and meteorological factors in Gansu Province. All four meteorological factors are negatively correlated with the number of influenza cases, the correlation between monthly average temperature and the number of influenza cases is the strongest ($r = -0.9$, $p < 0.01$), and the correlation between monthly total sunshine time and the number of influenza cases is the weakest ($r = -0.31$, $p < 0.01$). In particular, we find a high correlation between monthly total precipitation and the number of influenza cases ($r = -0.86$, $p < 0.01$), and a moderate correlation between monthly average relative humidity and the number of influenza cases ($r = -0.41$, $p < 0.01$). Figure 3a shows that the monthly total sunshine time is weakly correlated with the number of influenza cases; therefore, the effects of monthly total sunshine time are not considered in our model. Next, we use the sine function and the cosine function to fit the other three types of meteorological factors. In order

to unify the measurement units of several types of meteorological factors, we unitize the data of meteorological factors. Next, we use the least squares method to fit the meteorological factors, as shown in Fig. 3b–d.

Figure 3b shows the fitting effect of monthly average temperature; the fitting function is expressed as follows

$$T(t) = 0.6050 \sin\left(\frac{\pi}{6}t - 2.0364\right) + 0.3950. \tag{15}$$

Figure 3c shows the fitting effect of monthly average relative humidity; the fitting function is expressed as follows

$$H(t) = 0.2600 \cos\left(\frac{\pi}{6}t + 1.5138\right) + 0.7400. \tag{16}$$

Figure 3d shows the fitting effect of monthly total precipitation; the fitting function is expressed as follows

$$P(t) = 0.3089 \sin\left(\frac{\pi}{6}t + 16.7236\right) + 0.3119. \tag{17}$$

where $\pi/6$ represents $2\pi/12$ in Eqs. (15)–(17), that is, the period is 12 months.

3.3 Parameter Estimation and Model Fitting

We don't have reliable data on the rate of transmission and the influenza virus, and here we only consider the rate of influenza transmission and the rate of flu virus clearance. The key is to reasonably choose the functions $\beta(t)$, $\rho(t)$ and $\mu(t)$. According to the periodic characteristics of influenza in Gansu Province, we define the periodic direct transmission rate between susceptible individuals and infected individuals as follows

$$\beta(t) = \beta_0 + \beta_1 \sin\left(\frac{\pi}{6}t + \phi\right),$$

where $\pi/6$ means $2\pi/12$, that is, the period is 12 months, β_0 and β_1 indicate coefficient of direct transmission rate between susceptible individuals and infected individuals, ϕ indicates the phase of the T-periodic function. Periodic indirect transmission rates between susceptible individuals and infected individuals are defined as follows

$$\rho(t) = \rho_0 + \rho_1 \sin\left(\frac{\pi}{6}t + \phi\right),$$

where $\pi/6$ means $2\pi/12$, that is, the period is 12 months, ρ_0 and ρ_1 indicate coefficient of indirect transmission rate between susceptible individuals and infected individuals, ϕ indicates the phase of the T-periodic function. As we said in Introduction, cool and dry conditions can improve the survival rate and transmission rate of influenza virus in temperate regions (Sooryanarain and Elankumaran 2015), and the temperature decay rate of influenza virus in the environment is described as $\delta(T) = \alpha e^{\gamma T}$ (Handel et al.

2013), where T is the temperature and α and γ are constants. Therefore, we define the periodic clearance rate of influenza virus as follows

$$\mu(t) = \mu_0 \mathrm{e}^{\alpha_1 T(t) + \alpha_2 H(t) + \alpha_3 P(t)},$$

where $T(t)$, $H(t)$ and $P(t)$ are both periodic functions, μ_0 indicates the basic clearance rate of influenza virus, α_1 indicates the trade-off factor of temperature affecting virus clearance rate, α_2 indicates the trade-off factor of relative humidity affecting virus clearance rate, α_3 indicates the trade-off factor of precipitation affecting virus clearance rate.

In order to simulate the number of new cases of influenza in Gansu Province, the rationality of the model is verified by the number of cases actually monitored. Therefore, we mainly focus on cumulative infections and new infections every month in Gansu Province. Cumulative infection cases can be expressed as follows

$$\frac{\mathrm{d}C_C}{\mathrm{d}t} = \delta\sigma E + \kappa I_N, \quad \frac{\mathrm{d}C_N}{\mathrm{d}t} = (1-\delta)\sigma E - \kappa I_N,$$

where $C_C(t)$ indicates the number of cumulative infections of reported infected individuals, and $C_N(t)$ indicates the number of cumulative infections of unreported infected individuals.

As for the newly infected cases, it can be expressed as follows

$$P_C = C_C(t) - C_C(t-1), \tag{18}$$
$$P_N = C_N(t) - C_N(t-1), \tag{19}$$

where P_C and P_N represent the number of new cases of reported infected individuals and the number of new cases of unreported infected individuals, respectively, and t is regarded as month in the simulations. In what follows, we use Eq. (18) to fit the number of new cases of reported infected individuals in Gansu Province.

In the past seven years or so, many people have been infected with influenza in Gansu Province (see Fig. 4 for more accurate statistical results). In order to calculate the basic reproduction number R_0 of influenza in Gansu Province and predict changes in the next few years, it is necessary to estimate the unknown parameters of model (1) since several parameters and initial values of model (1) are assigned values based on existing data and experience (see Table 2). Next, we estimate all the parameters and initial values of model (1) in detail:

(i) the recruitment rate of susceptible (i.e., Λ): We obtain that the birth rate in Gansu Province at the end of 2011 is 12.08 per thousand by looking up the relevant data of the Gansu Provincial Bureau of Statistics (2019); at the same time, we also get the total population of Gansu Province at the end of 2011 is 25.813 million. Therefore, we can get a simple calculation that the monthly birth population of Gansu Province is about 25813;

(ii) the natural mortality rate of the population (i.e., d): According to the statistics of the National Bureau of Statistics of China (2019a), we conclude that the monthly natural mortality rate of the population in Gansu Province in 2012 is approximately

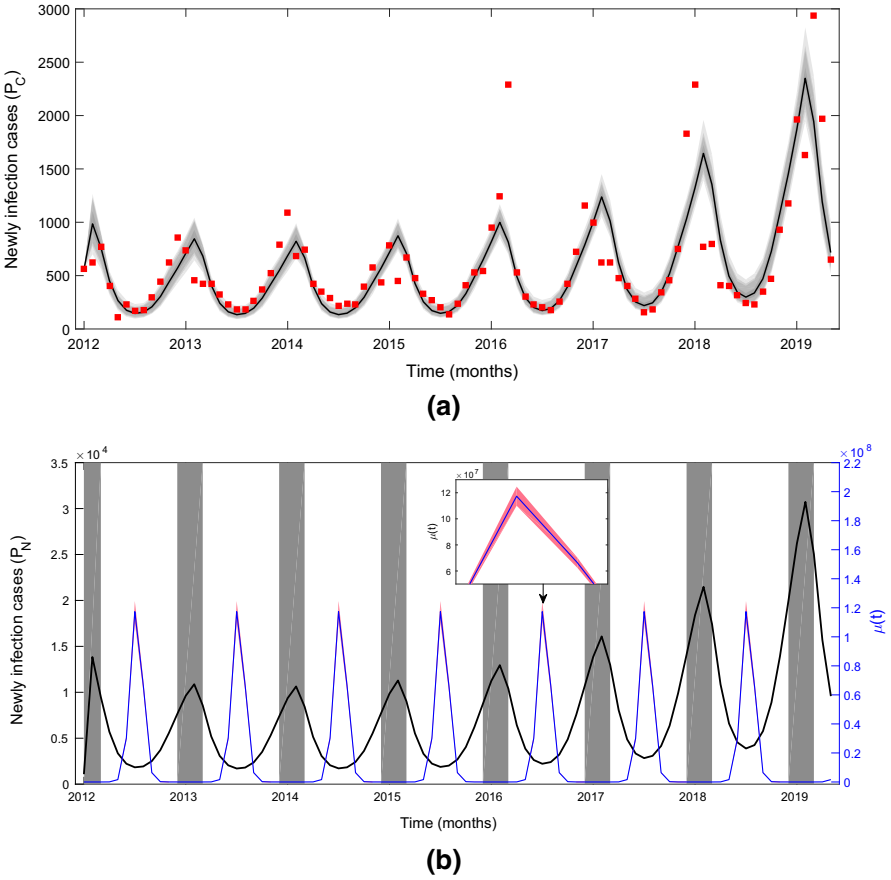

Fig. 4 **a** The fitting results of the number of new cases reported from January 2012 to May 2019. The solid black line represents the fitted data, and the red dots represent the actual data. The areas from the darkest to the lightest correspond to the 50%, 90%, 95% and 99% posterior limits of the model uncertainty. **b** The fitting result of the number of new cases not reported from January 2012 to May 2019. The blue curve represents the clearance rate $\mu(t)$, and the pink area represents 95% confidence interval. The gray area indicates December, January and February each year (For an explanation of the reference to color in this illustration, the reader is referred to the Web version of this article) (Color figure online)

$d = 1/(73 \times 12)$, where the constant 73 represents the average life expectancy of the population of Gansu Province;

(iii) the recovery rate of reported infected individuals (i.e., γ_1): We assume that the average recovery time of reported influenza patients is 7 days (Massad et al. 2007; Xing et al. 2017), then the recovery rate is $30/7$;

(iv) the recovery rate of unreported infected individuals (i.e., γ_2): We assume that the average recovery time of unreported influenza patients is 10 days (Massad et al. 2007; Xing et al. 2017), then the recovery rate is $30/10$;

(v) the mean incubation period (i.e., $1/\sigma$): The incubation period for influenza varies in different books, from a few hours to four days, the most common being three

Table 2 The parameters values and initial values of the model (1)

Parameters	Mean value	Std	95% CI	Reference
Λ	25813	–	–	(i)
d	$1/(73 \times 12)$	–	–	(ii)
γ_1	30/7	–	–	(iii)
γ_2	30/10	–	–	(iv)
σ	30/4	–	–	(v)
q	0.9	–	–	(vi)
β_0	1.7004×10^{-7}	1.5328×10^{-9}	$[1.6995 \times 10^{-7}, 1.7014 \times 10^{-7}]$	MCMC
β_1	3.7439×10^{-8}	3.9166×10^{-9}	$[3.7195 \times 10^{-8}, 3.7682 \times 10^{-8}]$	MCMC
ρ_0	7.2955×10^{-9}	6.6911×10^{-10}	$[7.2540 \times 10^{-9}, 7.3371 \times 10^{-9}]$	MCMC
ρ_1	9.7260×10^{-10}	1.0705×10^{-9}	$[9.0617 \times 10^{-10}, 1.0390 \times 10^{-9}]$	MCMC
ϕ	2.6882	0.1051	[2.6817, 2.6947]	MCMC
θ	0.3184	0.03324	[0.3163, 0.3205]	MCMC
δ	0.04211	3.8964×10^{-3}	[0.04186, 0.04235]	MCMC
α	259.4835	47.1153	[256.5598, 262.4072]	MCMC
μ_0	32.7373	2.8047	[32.5633, 32.9114]	MCMC
α_1	7.6908	0.6667	[7.6494, 7.7321]	MCMC
α_2	4.2128	0.3497	[4.1911, 4.2345]	MCMC
α_3	5.4728	0.2831	[5.4552, 5.4903]	MCMC
κ	0.09102	0.003304	[0.09081, 0.09123]	MCMC
$S(0)$	18,295,942	1,586,759	[18,197,594, 18,394,290]	MCMC
$E(0)$	579	63	[575, 583]	MCMC
$I_N(0)$	1083	31	[1081, 1085]	MCMC
$I_C(0)$	562	–	–	(vii)
$R(0)$	2706	404	[2681, 2731]	MCMC
$V(0)$	2,643,292	2,146,411	[2,510,256, 2,776,328]	MCMC

to four days (Lancet 1918). In this paper, we assume that the average incubation time is 4 days; then monthly, the average incubation period $1/\sigma$ can be determined by $4/30$;

(vi) the progression rate of the recovered individuals (i.e., q): In this paper, we assume that the progression rate of the recovered individuals is $q = 0.9$;

(vii) the initial value of the reported influenza cases (i.e., $I_C(0)$): According to the relevant data reported by the Gansu Provincial Center for Disease Control and Prevention (2019), we obtain the initial value of $I_C(t)$ as 562;

(viii) The other parameters and initial values of model (1) are estimated by the MCMC algorithm, as shown in Table 2.

We use MATLAB 2016b software to fit the unknown parameters and initial values of model (1). In this article, we use an adaptive combination Delayed rejection and Adaptive Metropolis (DRAM) algorithm to carry out the Markov chain Monte Carlo (MCMC) procedure (Haario et al. 2001, 2006). Here, the MCMC toolbox is provided by a website (Laine 2019). The algorithm runs 10,000 iterations and uses the Geweke

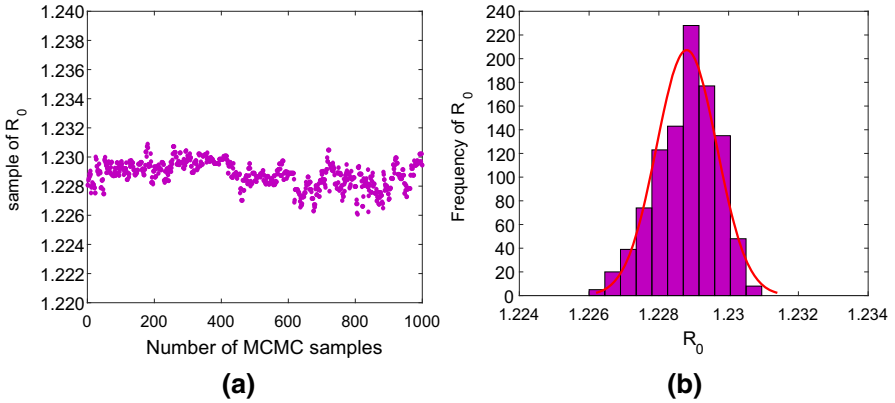

Fig. 5 **a** The Markov chain of the last 1000 samples of R_0. The purple dot represents the size of the R_0 value. **b** The frequency distribution of R_0. The red curve is the probability density function curve of R_0 (For an explanation of the reference to color in this illustration, the reader is referred to the Web version of this article) (Color figure online)

convergence diagnostic method to evaluate chain convergence (Haario et al. 2006). We can estimate the convergence of the Markov chain by the closeness of the Geweke value to 1. The mean, standard deviation and 95% confidence interval of the estimated parameters are shown in Table 2, and the fitting result can be seen in Fig. 4a.

It can be seen from Fig. 4a that our fitting effect is good. According to the two fitting curves of Fig. 4, it can be seen that influenza in Gansu Province is on an annual upward trend. In addition, we also obtain that the number of unreported influenza cases is much higher than the number of reported influenza cases. According to the parameters in Table 2, we can use the theory developed by Wang and Zhao (2008) to calculate the basic reproduction number with the periodic model (1). The basic reproduction number R_0 can be calculated by Lemma 2.3.2(2), and R_0 is estimated to be 1.2288 (95% CI:(1.2287, 1.2289)), as shown in Fig. 5. This means that influenza in Gansu Province is impossible to ignore. It can be seen from Fig. 5b that the basic reproduction number R_0 is normally distributed. Therefore, we can easily get the confidence interval and mean of R_0. Furthermore, it follows from Fig. 4b that the number of influenza cases peaks when the rate of influenza virus clearance is lowest; this means that meteorological factors are the dominant factor in the seasonal outbreak of influenza.

4 Uncertainty and Sensitivity Analysis

As we discussed in Introduction, the periodicity of influenza in Gansu Province may be related to factors such as temperature, relative humidity, and precipitation. However, it is unclear which one is internal and the main factor. Now let us observe the respective effects of each meteorological factor.

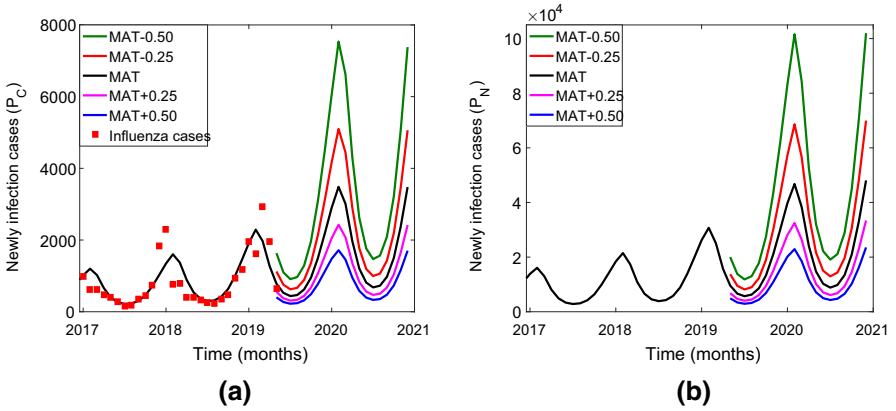

Fig. 6 The goodness of fit and prediction of the dynamic trend of influenza infection with temperature as an intervention. **a** The trend of announced influenza cases affected by the change of monthly average temperature. **b** The trend of unannounced influenza cases affected by the change of monthly average temperature (For an explanation of the reference to color in this illustration, the reader is referred to the Web version of this article) (Color figure online)

Table 3 The number of new cases has changed due to changes in monthly average temperature (MAT)

Meteorological factors variation	MAT-0.50	MAT-0.25	MAT	MAT+0.25	MAT+0.50
Forecasting the number of new cases in December 2019	66,552	46,124	32,310	23,007	16,653
Increased by a rate	105.98%	42.75%	0%	− 28.79%	− 48.46%
Forecasting the number of new cases in January 2020	89,233	61,386	42,651	30,132	21,641
Increased by a rate	109.22%	43.92%	0%	− 29.35%	− 49.26%
Forecasting the number of new cases in February 2020	109,150	73,718	50,252	34,905	24,645
Increased by a rate	117.21%	46.70%	0%	− 30.54%	− 50.96%

4.1 Sensitivity of MAT to Influenza Cases and Basic Reproduction Number

According to the parameters estimated in Table 2, the number of influenza cases will decrease by 48.46% and 28.79% as the monthly average temperature (MAT) increases by 0.5°C and 0.25 °C in December 2019, respectively. At the same time, the number of influenza cases will increase by 105.98% and 42.75% as the monthly average temperature (MAT) decreases by 0.5°C and 0.25°C in December 2019, respectively, as shown in Fig. 6 and Table 3. More predictions of the impact of warming measures on influenza cases in January 2020 and February 2020 are summarized in Table 3. The variation of R_0 with temperature was studied by simulation. Obviously, as the monthly average temperature (MAT) increases, R_0 gradually decreases, as shown in Fig. 9.

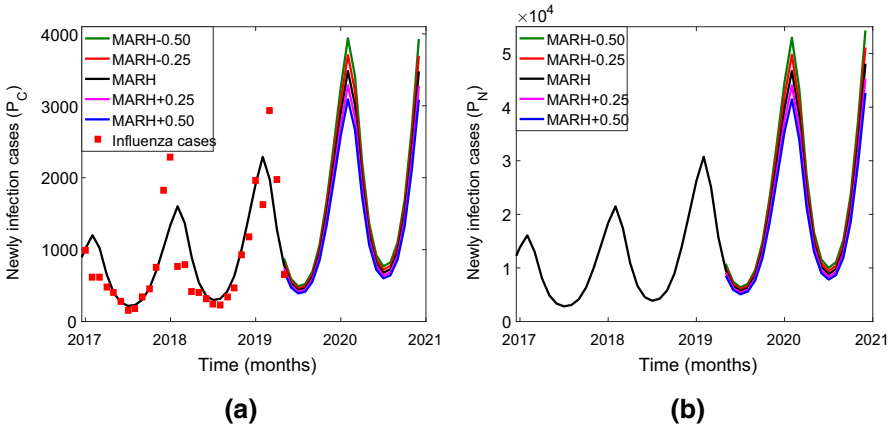

Fig. 7 The goodness of fit and prediction of the dynamic trend of influenza infection with relative humidity as an intervention. **a** The trend of announced influenza cases affected by the change of monthly average relative humidity. **b** The trend of unannounced influenza cases affected by the change of monthly average relative humidity (For an explanation of the reference to color in this illustration, the reader is referred to the Web version of this article) (Color figure online)

Table 4 The number of new cases has changed due to changes in monthly average relative humidity (MARH)

Meteorological factors variation	MARH-0.50	MARH-0.25	MARH	MARH+0.25	MARH+0.50
Forecasting the number of new cases in December 2019	36,236	34,221	32,310	30,564	28,875
Increased by a rate	12.15%	5.91%	0%	− 5.40%	− 10.63%
Forecasting the number of new cases in January 2020	47,961	4.5238	42,651	40,292	38,015
Increased by a rate	12.45%	6.06%	0%	− 5.53%	− 10.87%
Forecasting the number of new cases in February 2020	56,884	53,469	50,252	47,355	44,546
Increased by a rate	13.20%	6.40%	0%	−5.76%	−11.35%

4.2 Sensitivity of MARH to Influenza Cases and Basic Reproduction Number

In comparison, our simulations also shows that the number of influenza cases will decrease by 10.63% and 5.40% as the monthly average relative humidity (MARH) increases by 0.5% and 0.25% in December 2019, respectively. At the same time, the number of influenza cases will increase by 12.15% and 5.91% as the monthly average relative humidity (MARH) decreases by 0.5% and 0.25% in December 2019, respectively, as shown in Fig. 7 and Table 4. More predictions of the impact of changing relative humidity on influenza cases in January 2020 and February 2020 are summarized in Table 4. The change of the basic reproduction number R_0 with the monthly average relative humidity (MARH) is shown in Fig. 9. We can see that R_0 gradually decreases with increasing monthly average relative humidity (MARH).

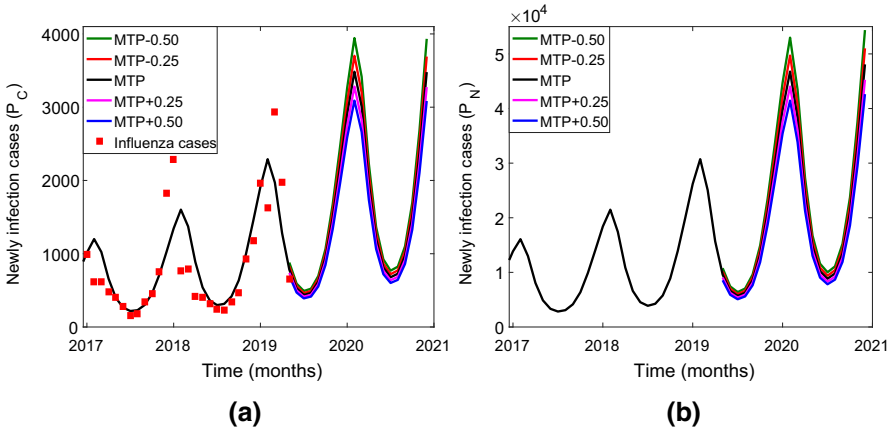

Fig. 8 The goodness of fit and prediction of the dynamic trend of influenza infection with precipitation as an intervention. **a** The trend of announced influenza cases affected by the change of monthly total precipitation. **b** The trend of unannounced influenza cases affected by the change of monthly total precipitation (For an explanation of the reference to color in this illustration, the reader is referred to the Web version of this article) (Color figure online)

Table 5 The number of new cases has changed due to changes in monthly total precipitation (MTP)

Meteorological factors variation	MTP-0.50	MTP-0.25	MTP	MTP+0.25	MTP+0.50
Forecasting the number of new cases in December 2019	36, 263	34, 158	32, 310	30, 539	28, 867
Increased by a rate	12.23%	5.72%	0%	−5.48%	−10.66%
Forecasting the number of new cases in January 2020	47, 994	45, 156	42, 651	40, 346	38, 006
Increased by a rate	12.53%	5.87%	0%	−5.40%	−10.89%
Forecasting the number of new cases in February 2020	56, 923	53, 401	50, 252	47, 309	44, 540
Increased by a rate	13.28%	6.27%	0%	−5.85%	−11.37%

4.3 Sensitivity of MTP to Influenza Cases and Basic Reproduction Number

In order to investigate effect of monthly total precipitation (MTP) on the number of influenza cases, we find that the number of influenza cases will decrease by 10.66% and 5.45% as the monthly total precipitation (MTP) increases by 0.5mm and 0.25mm in December 2019, respectively. At the same time, the number of influenza cases will increase by 12.23% and 5.72% as the monthly total precipitation (MTP) decreases by 0.5mm and 0.25mm in December 2019, respectively, as shown in Fig. 8 and Table 5. More predictions of the impact of changing precipitation on influenza cases in January 2020 and February 2020 are summarized in Table 5. In addition, we also find that R_0 decreases with increasing monthly total precipitation (MTP), as shown in Fig. 9.

Figures 6, 7 and 8 show the number of predicted influenza individuals. It shows that an increase in the value of meteorological factors leads to a reduction in influenza indi-

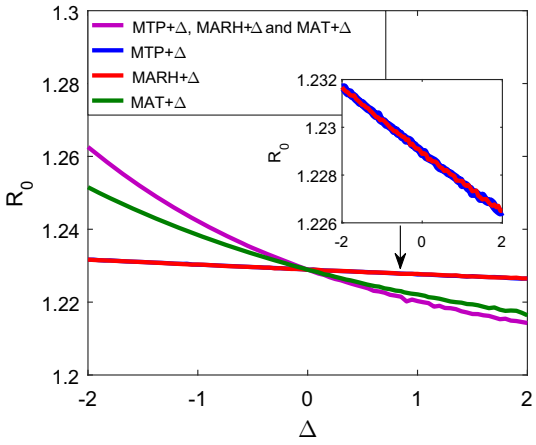

Fig. 9 The influence of meteorological factors on R_0, the green curve represents the measure to change the temperature, the red curve represents the measure to change the relative humidity, the blue curve represents the measure to change the precipitation, and the purple curve represents the measure of the simultaneous change of the three meteorological factors (For an explanation of the reference to color in this illustration, the reader is referred to the Web version of this article) (Color figure online)

viduals and then reduces the severity of influenza. This means that increasing indoor temperature and air humidity during the high season of influenza plays an important role in reducing the number of infected individuals and promoting effective disease control. For example, it is necessary to install air conditioners and air humidifiers indoors in winter. This is consistent with the findings of Kudo et al. (2019). In particular, as can be seen from Figs. 7 and 8, we can obtain that the two meteorological factors of precipitation and relative humidity have almost the same effect on influenza, which is consistent with our experience. By comparing the data in Tables 3, 4 and 5, we obtain that temperature has a greater impact on influenza than relative humidity and precipitation, so the seasonal change in temperature is a major factor in the seasonal outbreak of influenza in Gansu Province, which is consistent with the conclusions in Lowen et al. (2007). At the same time, the effects of relative humidity and precipitation cannot be ignored. Then, we also note that R_0 changes most significantly under the combined action of three meteorological factors. This means that air conditioners and air humidifiers should be used simultaneously during periods of high influenza. In addition, we obtain that temperature is the main influencing factor of influenza, and the relative humidity and precipitation have almost the same effect on R_0, which is consistent with the above conclusion.

4.4 Sensitivity of $\beta(t)$, $\rho(t)$ and $\mu(t)$ to Influenza Cases and Basic Reproduction Number

In order to study the effects of human-to-human contact transmission rate, human-to-pollutant contact transmission rate and influenza virus clearance rate on influenza, we investigate the changes of new cases and basic reproduction number with $\beta(t)$, $\rho(t)$, and $\mu(t)$. Figure 10a–d shows the number of predicted new cases of individuals and basic reproduction number. It shows that a decrease in transmission rate or an increase in clearance rate leads to a decrease in new infections and then a reduction in the severity of influenza. This means that health precautions and environmental cleansing play an important role in reducing the number of infected individuals and

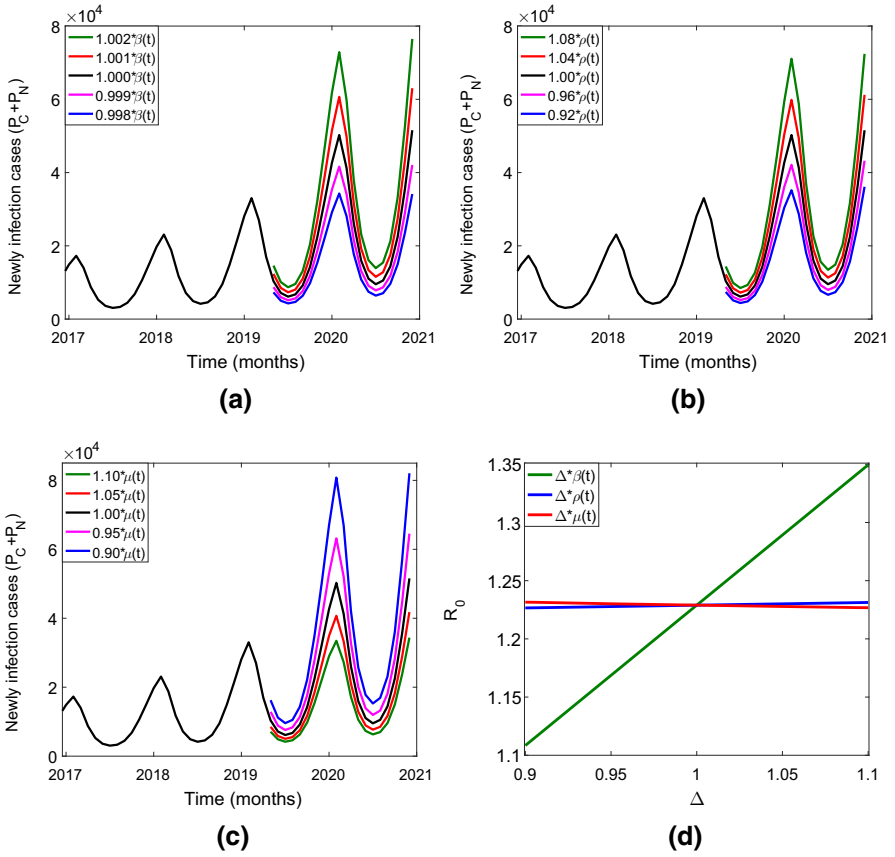

Fig. 10 **a** The effect of changes in direct transmission rate $\beta(t)$ on the number of new cases. **b** The effect of changes in the indirect transmission rate $\rho(t)$ on the number of new cases. **c** The effect of pathogen clearance rate $\mu(t)$ on the number of new cases. **d** The trend chart of basic reproduction number R_0 varies with $\beta(t)$, $\rho(t)$ and $\mu(t)$ (For an explanation of the reference to color in this illustration, the reader is referred to the Web version of this article) (Color figure online)

promoting effective disease control. For example, influenza patients should pay attention to personal hygiene and other public health measures. In particular, as can be seen from Fig. 10c, we can obtain the impact of the environment on influenza, that is, the polluted environment greatly contributes to new infections and increases the risk of disease transmission. By comparing the blue and green curves in Fig. 10a, d with b, we obtain that the direct transmission rate has a greater impact on new cases and basic reproduction number than the indirect transmission rate. This means that the direct transmission rate has a significant impact on influenza outbreaks and transmission.

4.5 Sensitivity of Other Parameters to Influenza Cases and Basic Reproduction Number

In what follows, we use the Latin hypercube sampling (LHS) and the partial rank correlation coefficient (PRCC) to study the global uncertainty and sensitivity of the other parameters of the model (1) (Marino et al. 2008). According to the estimation results of the parameters in Table 2, we select a normal distribution for all input parameters, where the mean and standard deviation are given in Table 2. The values of PRCCs are calculated for multiple time points and plotted against time. This allows us to assess the importance of the parameters over the entire time period. A positive (or negative) PRCC value indicates a positive (or negative) correlation between the input parameter and the output variable. The absolute value of PRCC between 0 and 0.2 indicates that there is no significant correlation between the input parameters and the output variables. The absolute value of PRCC between 0.2 and 0.4 indicates the moderate correlation between the input parameters and the output variables. The absolute value of PRCC between 0.4 and 1 indicates the high correlation between the input parameters and the output variables.

Figure 11a and b shows 5000 sample fits of the model (1) output variables P_C and P_N from January 2012 to May 2019. We can see that the 5000 simulations of the output variables P_C and P_N are periodic, which reflects the periodicity of influenza in Gansu Province. From Fig. 11c and d, it can be seen that the changes in several parameters over time have an impact on reported new cases and unreported new cases. In particular, there is strong negative correlation between the basic clearance rate μ_0 and the number of new cases. This means that the public health department should strengthen the disinfection work. There is also strong negative correlation between the reported rate δ and the number of new cases. This means that the Gansu Provincial Center for Disease Control and Prevention can suppress the spread of influenza by increasing the reporting rate. There is moderate negative correlation between the treatment rate κ of unreported cases and the number of new cases. This suggests that patients with influenza should go to the hospital for treatment rather than family treatment, especially in poor areas like Gansu. Then, parameters α and θ are strongly positively correlated throughout the time period. This indicates that the self-protection measures of influenza patients and the therapeutic effects of medical institutions cannot be ignored.

In the case of the above LHS (Latin hypercube sampling) matrix, we evaluate the sensitivity of the output variable R_0 and various input parameters (e.g., β_0, β_1, δ, θ, ρ_0, ρ_1, α, μ_0, κ) by the PRCC. Figure 12a shows the sampling result of R_0 by the LHS (Latin hypercube sampling) method, and Fig. 12b shows the distribution of R_0 and the probability density function curve. Figure 12c shows the sensitivity of R_0 to each parameter. The goal is to determine the most important parameters affecting influenza dynamics based on the basic reproduction number. Our results indicate that the parameters strongly correlated with R_0 are the coefficient β_0 of direct transmission rate, the virus shedding rate α, the reporting rate δ, the basic clearance rate of pathogens μ_0, the modification factor θ and the coefficient ρ_0 of indirect transmission rate. Therefore, our results provide possible interventions to reduce influenza infections, such as reducing out-of-town and exposure during periods of high influenza influenza,

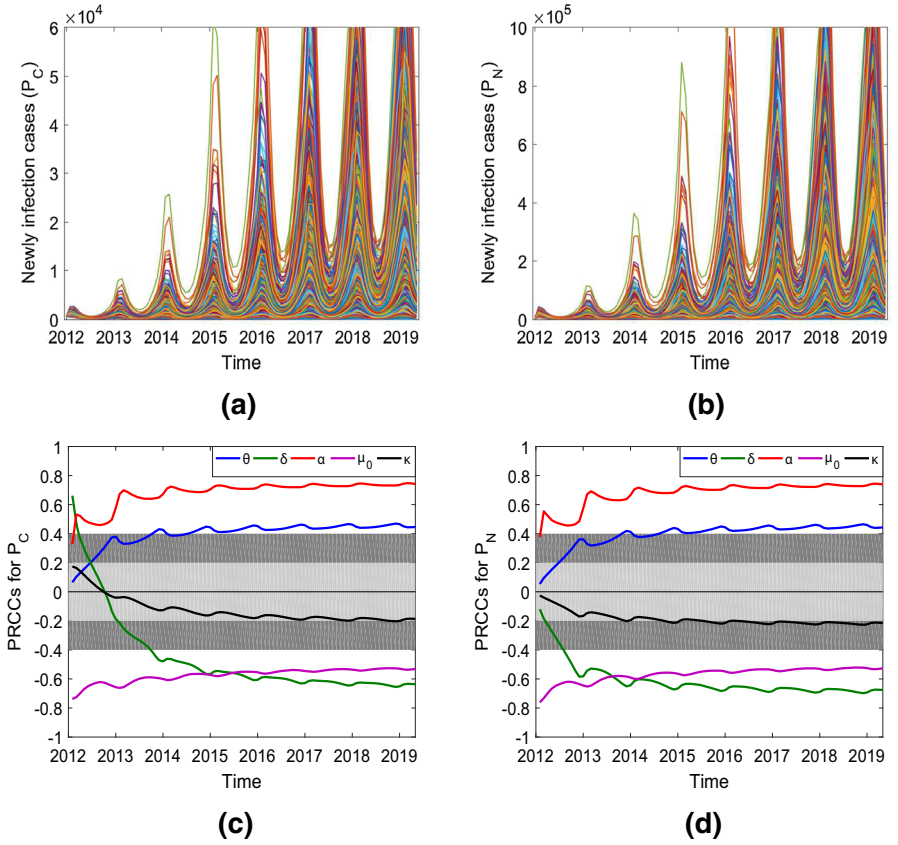

Fig. 11 Sensitivity analysis. **a** Plot of the output (5000 runs) of model (1). The ordinate represents variable $P_C(t)$, and the abscissa represents time (months). **b** Plot of the output (5000 runs) of model (1). The ordinate represents variable $P_N(t)$, and the abscissa represents time (months). **c** and **d** The sensitivity of the parameters changes as the dynamics of model (1) progress. The light gray area represents PRCC values that are not statistically significant. The dark gray areas represent PRCC values that are moderate correlation (For an explanation of the reference to color in this illustration, the reader is referred to the Web version of this article) (Color figure online)

influenza patients and susceptible individuals wearing masks to reduce influenza virus transmission through droplets, the public health sector Increase coverage of influenza, and increase the frequency of disinfection in healthcare facilities. In addition, the parameters κ and R_0 are moderately negatively correlated, which suggests that we should go to hospital for treatment regardless of whether the influenza is serious or not.

The variation of R_0 is studied by simulating the changes of parameters κ and θ, as shown in Fig. 13a. It is obvious that R_0 is decreasing as the parameter κ increases and θ decreases. Note that the number of treatments for influenza patients reflects an increase in parameter κ, while the treatment effect in the health sector reflects a decrease in parameter θ. The variation charts of R_0 with parameters α and μ_0 show that the increase in parameter α and the decrease in parameter μ_0 lead to the increase

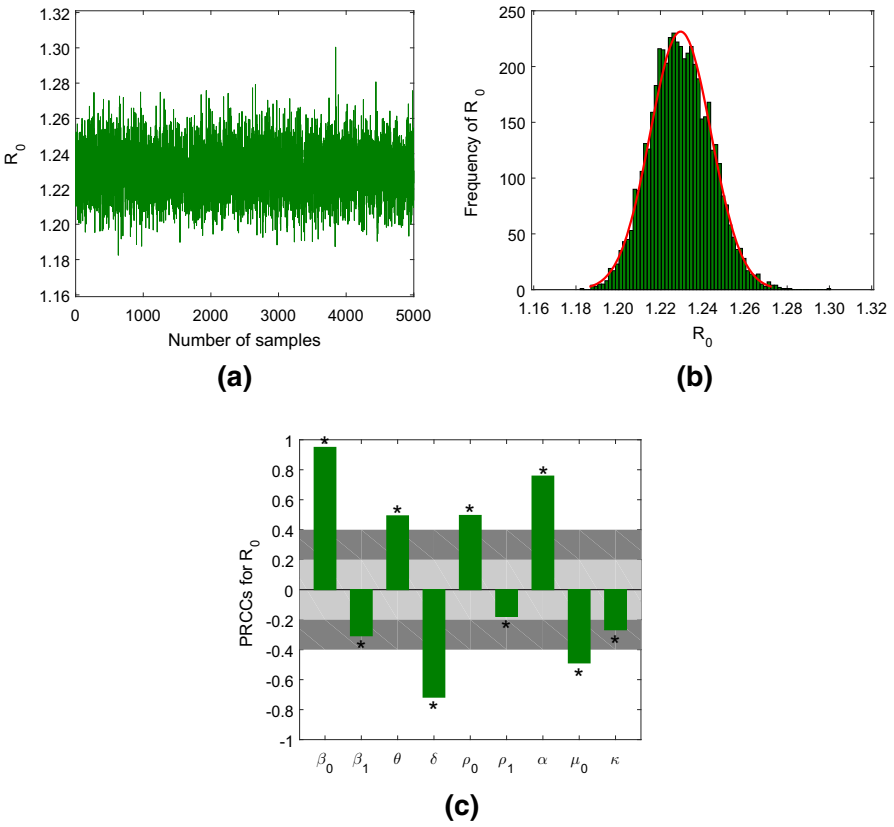

Fig. 12 **a** The number of samples of R_0 is obtained by the LHS (Latin hypercube sampling) method. **b** The distribution of R_0 is obtained by the LHS (Latin hypercube sampling) method. **c** The PRCC results for the dependence of R_0 on each parameter. The light gray area represents PRCC values that are not statistically significant. The dark gray areas represent PRCC values that are moderate correlation. $*$ indicates that the impact of the parameters is significant, where the significance level is 0.05 (For an explanation of the reference to color in this illustration, the reader is referred to the Web version of this article) (Color figure online)

in R_0, which reflects the effect of pathogen density on R_0 in the environment, as shown in Fig. 13b.

5 Conclusion and Discussion

In this paper, in order to study the dynamic relationship among meteorological factors, unreported cases and influenza, we propose a new non-autonomous differential equation model (1) with meteorological factors and unreported cases. The basic reproduction number is obtained. The global asymptotic stability of the disease-free periodic solution is proved. The existence of the periodic solution and the uniformly persistence of model (1) are also derived. We use the MCMC algorithm to estimate the unknown

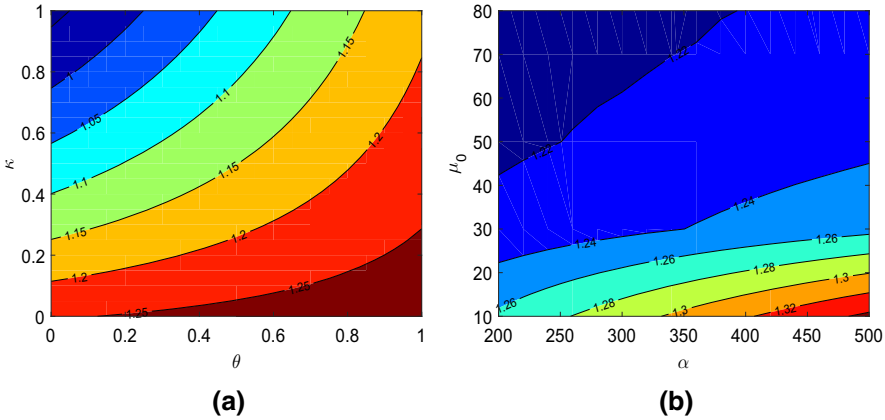

Fig. 13 Plots of R_0 for model (1) with κ, θ, α and μ_0. **a** Contour plot of R_0 when κ and θ vary. **b** Contour plot of R_0 when α and μ_0 vary (For an explanation of the reference to color in this illustration, the reader is referred to the Web version of this article) (Color figure online)

parameters and initial values of model (1) on the basis of the influenza data in Gansu province, China. The uncertainty and sensitivity of all parameters are evaluated by using the Latin hypercube sampling (LHS) and the partial rank correlation coefficient (PRCC).

Through the mean and confidence intervals of the parameters in Table 2, we obtain the basic reproduction number $R_0 = 1.2288$ (95% CI:(1.2287, 1.2289)), which means that influenza is still pandemic in the crowd. The sensitivity of the parameters provides a possible intervention to reduce influenza infection. Infected individuals and susceptible individuals should wear masks or reduce their outings to reduce the spread of influenza viruses through droplets during influenza outbreaks (i.e., reducing the value of the parameters $\beta(t)$ and α). Susceptible individuals and recovery individuals should reduce exposure to contaminated items by wearing gloves (i.e., reducing the value of the parameter $\rho(t)$). Public health departments should increase the reporting rate for influenza patients (i.e., increasing the value of the parameter δ). The therapeutic effect of medical institutions should be improved (i.e., reducing the value of the parameter θ). The hospital should disinfect contaminated items during the high season of influenza (i.e., the more the value of the parameter μ_0). In particular, unreported influenza patients should go to the hospital for treatment rather than staying at home for treatment (i.e., increasing the value of the parameter κ).

In addition, our results show that influenza is more likely to spread in winter in Gansu. When relative humidity, temperature and precipitation reduce, the incidence and mortality of influenza rise. Therefore, we know that relative humidity, temperature and precipitation are the main factors in the outbreak of influenza in winter in Gansu. The use of humidifiers and air conditioners in hospital, school or home can increase humidity and temperature, which means can reduce the risk of transmission of influenza.

It follows from Fig. 4a that the number of influenza cases is increasing every year in Gansu. Some reasons may bring this phenomenon, such as air pollution, travel

frequency, and population migration. Then considering the effect of these factors and exploring the occurrence of increasing influenza cases every year should be interesting, and we leave these work for future.

Acknowledgements This work is supported by the National Natural Science Foundation of China (11861044 and 11661050) and the HongLiu first-class disciplines Development Program of Lanzhou University of Technology.

Compliance with ethical standards

Conflict of interest The authors declare that they have no conflict of interest.

Appendix A

See Figs. 14 and 15.

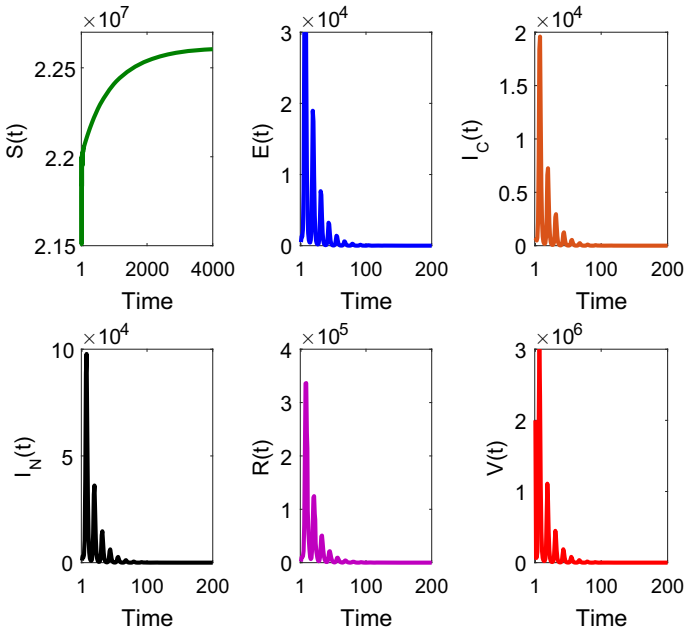

Fig. 14 Numerical simulation of the global stability of the disease-free periodic solution P_0, where the values of the parameters are $\beta(t) = 6.4 \times 10^{-8} + 8 \times 10^{-10} \sin(\frac{\pi}{6}t + 2)$, $\theta = 0.3$, $\delta = 0.2$, $\rho(t) = 6.4 \times 10^{-9} + 9 \times 10^{-10} \sin(\frac{\pi}{6}t + 2)$, $\alpha = 590$, $\mu(t) = 32 + 20 \sin(\frac{\pi}{6}t + 2)$, $\kappa = 0.09$, $\Lambda = 25813$, $d = 1/(73 \times 12)$, $q = 0.9$, $\sigma = 30/4$, $\gamma_1 = 30/7$ and $\gamma_2 = 30/10$. The initial value of model (1) is $(S(0), E(0), I_C(0), I_N(0), R(0), V(0)) = (22,000,000,500,500,1000,2000,20,00,000)$. According to this set of parameters, we get $R_0 = 0.99127 < 1$ (For an explanation of the reference to color in this illustration, the reader is referred to the Web version of this article)

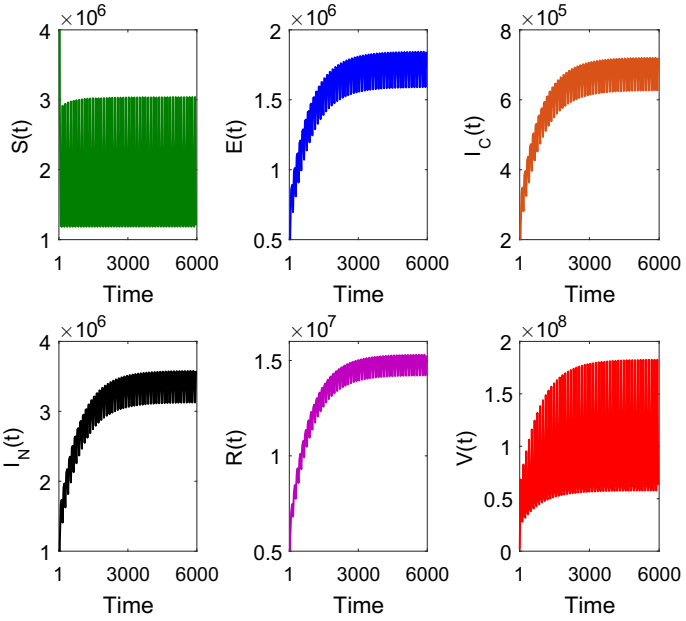

Fig. 15 The existence of the positive periodic solution, where the values of the parameters are $\beta(t) = 7 \times 10^{-7} + 8 \times 10^{-8} \sin(\frac{\pi}{6}t + 2)$, $\theta = 0.3$, $\delta = 0.2$, $\rho(t) = 1 \times 10^{-7} + 9 \times 10^{-8} \sin(\frac{\pi}{6}t + 2)$, $\alpha = 590$, $\mu(t) = 32 + 20 \sin(\frac{\pi}{6}t + 2)$, $\kappa = 0.09$, $\Lambda = 25813$, $d = 1/(73 \times 12)$, $q = 0.9$, $\sigma = 30/4$, $\gamma_1 = 30/7$ and $\gamma_2 = 30/10$. The initial value of model (1) is $(S(0), E(0), I_C(0), I_N(0), R(0), V(0)) = (10, 000, 000, 500, 500, 1000, 2000, 20, 00, 000)$. According to this set of parameters, we get $R_0 = 15.4955 > 1$ (For an explanation of the reference to color in this illustration, the reader is referred to the Web version of this article) (Colour figure online)

References

Aronsson G, Kellogg RB (1978) On a differential equation arising from compartmental analysis. Math Biosci 38(1):113–122

Bao XX, Li WT (2020) Propagation phenomena for partially degenerate nonlocal dispersal models in time and space periodic habitats. Nonlinear Anal Real World Appl. https://doi.org/10.1016/j.nonrwa.2019.102975

Bao XX, Li WT, Wang ZC (2020) Uniqueness and stability of time-periodic pyramidal fronts for a periodic competition–diffusion system. Commun Pure Appl Anal 19:253–277

Ducrot A, Magal P, Nguyen T, Webb G (2019) Identifying the number of unreported cases in SIR epidemic models. Math Med Biol J IMA 37:243–261

Eccles R (2002) An explanation for the seasonality of acute upper respiratory tract viral infections. Acta Oto-laryngol 122(2):183–191

Foxman EF, Storer JA, Fitzgerald ME, Wasik BR, Hou L, Zhao H, Turner PE, Pyle AM, Iwasaki A (2015) Temperature-dependent innate defense against the common cold virus limits viral replication at warm temperature in mouse airway cells. Proc Natl Acad Sci 112(3):827–832

Gamado KM, Streftaris G, Zachary S (2014) Modelling under-reporting in epidemics. J Math Biol 69(3):737–765

Gamado K, Streftaris G, Zachary S (2017) Estimation of under-reporting in epidemics using approximations. J Math Biol 74(7):1683–1707

Gansu Provincial Bureau of Statistics (2019) Gansu Province statistical yearbook. http://www.gstj.gov.cn/. Accessed 8 Mar 2019

Gansu Provincial Center for Disease Control and Prevention (2019) Epidemic notification. http://www.gscdc.net/. Accessed 12 Mar 2019
Grubaugh ND, Saraf S, Gangavarapu K, Watts A, Tan AL, Oidtman RJ, Ladner JT, Oliveira G, Matteson NL, Kraemer MU et al (2019) Travel surveillance and genomics uncover a hidden zika outbreak during the waning epidemic. Cell 178(5):1057–1071
Guo ZK, Huo HF, Xiang H (2019) Global dynamics of an age-structured malaria model with prevention. Math Biosci Eng 16(3):1625–1653
Haario H, Saksman E, Tamminen J (2001) An adaptive metropolis algorithm. Bernoulli 7(2):223–242
Haario H, Laine M, Mira A, Saksman E (2006) DRAM: efficient adaptive MCMC. Stat Comput 16(4):339–354
Handel A, Brown J, Stallknecht D, Rohani P (2013) A multi-scale analysis of influenza A virus fitness trade-offs due to temperature-dependent virus persistence. PLoS Comput Biol 9(3):e1002989
Hirsch MW (1985) Systems of differential equations that are competitive or cooperative II: convergence almost everywhere. SIAM J Math Anal 16(3):423–439
Huo HF, Cui FF, Xiang H (2018) Dynamics of an SAITS alcoholism model on unweighted and weighted networks. Physica A Stat Mech Appl 496:249–262
Huo HF, Jing SL, Wang XY, Xiang H (2019a) Modelling and analysis of an alcoholism model with treatment and effect of twitter. Math Biosci Eng 16(5):3595–3622
Huo HF, Yang P, Xiang H (2019b) Dynamics for an sirs epidemic model with infection age and relapse on a scale-free network. J Frankl Inst 356:7411–7443
Kudo E, Song E, Yockey LJ, Rakib T, Wong PW, Homer RJ, Iwasaki A (2019) Low ambient humidity impairs barrier function and innate resistance against influenza infection. Proc Natl Acad Sci 116(22):10905–10910
Laine M (2019) MCMC toolbox for Matlab, report of Marko Laine. http://www.helsinki.fi/mjlaine/mcmc/. Accessed 15 Feb 2019
Lancet T (1918) The incubation period of influenza. Lancet 192(1595):635
Loosli C, Lemon H, Robertson O, Appel E (1943) Experimental air-borne influenza infection. I. Influence of humidity on survival of virus in air. Proc Soc Exp Biol Med 53(2):205–206
Lowen AC, Steel J (2014) Roles of humidity and temperature in shaping influenza seasonality. J Virol 88(14):7692–7695
Lowen AC, Mubareka S, Steel J, Palese P (2007) Influenza virus transmission is dependent on relative humidity and temperature. PLoS Pathog 3(10):e151
Ma ZP (2019) Spatiotemporal dynamics of a diffusive leslie-gower prey-predator model with strong alee effect. Nonlinear Anal Real World Appl 50:651–674
Magal P, Webb G (2018) The parameter identification problem for SIR epidemic models: identifying unreported cases. J Math Biol 77(6–7):1629–1648
Mäkinen TM, Juvonen R, Jokelainen J, Harju TH, Peitso A, Bloigu A, Silvennoinen-Kassinen S, Leinonen M, Hassi J (2009) Cold temperature and low humidity are associated with increased occurrence of respiratory tract infections. Respir Med 103(3):456–462
Marino S, Hogue IB, Ray CJ, Kirschner DE (2008) A methodology for performing global uncertainty and sensitivity analysis in systems biology. J Theor Biol 254(1):178–196
Massad E, Burattini MN, Coutinho FAB, Lopez LF (2007) The 1918 influenza A epidemic in the city of Sao Paulo, Brazil. Med Hypotheses 68(2):442–445
Meng XY, Wu YQ (2018) Bifurcation and control in a singular phytoplankton-zooplankton-fish model with nonlinear fish harvesting and taxation. Int J Bifurc Chaos 28(3):1850042
Mourtzoukou E, Falagas ME (2007) Exposure to cold and respiratory tract infections. The International Journal of Tuberculosis and Lung Disease 11(9):938–943
National Bureau of Statistics of China (2019a) Annual statistics of Gansu Province. http://data.stats.gov.cn/. Accessed 20 Mar 2019
National Bureau of Statistics of China (2019b) China statistical yearbook. http://www.stats.gov.cn/tjsj/ndsj/. Accessed 20 Mar 2019
National Health Commission of the People's Republic of China (2019) Overview of the national legal infectious disease epidemic in 2018. http://www.nhc.gov.cn/wjw/index.shtml. Accessed 27 Mar 2019
Pyankov OV, Bodnev SA, Pyankova OG, Agranovski IE (2018) Survival of aerosolized coronavirus in the ambient air. J Aerosol Sci 115:158–163
Shaman J, Pitzer VE, Viboud C, Grenfell BT, Lipsitch M (2010) Absolute humidity and the seasonal onset of influenza in the continental United States. PLoS Biol 8(2):e1000316

Smith HL, Waltman P (1995) The theory of the chemostat: dynamics of microbial competition, vol 13. Cambridge University Press, Cambridge
Sooryanarain H, Elankumaran S (2015) Environmental role in influenza virus outbreaks. Annu Rev Anim Biosci 3(1):347–373
Tamerius J, Nelson MI, Zhou SZ, Viboud C, Miller MA, Alonso WJ (2010) Global influenza seasonality: reconciling patterns across temperate and tropical regions. Environ Health Perspect 119(4):439–445
Tamerius JD, Shaman J, Alonso WJ, Bloom-Feshbach K, Uejio CK, Comrie A, Viboud C (2013) Environmental predictors of seasonal influenza epidemics across temperate and tropical climates. PLoS Pathog 9(3):e1003194
Tang S, Yan Q, Shi W, Wang X, Sun X, Yu P, Wu J, Xiao Y (2018) Measuring the impact of air pollution on respiratory infection risk in China. Environ Pollut 232:477–486
Viboud C, Alonso WJ, Simonsen L (2006) Influenza in tropical regions. PLoS Med 3(4):e89
Wang WD, Zhao XQ (2008) Threshold dynamics for compartmental epidemic models in periodic environments. J Dyn Differ Equ 20(3):699–717
Wang J, Xiao Y, Cheke RA (2016a) Modelling the effects of contaminated environments on hfmd infections in mainland China. Bio Syst 140(1–2):1–7
Wang J, Xiao Y, Peng Z (2016b) Modelling seasonal HFMD infections with the effects of contaminated environments in mainland China. Appl Math Comput 274:615–627
Xiang H, Zou MX, Huo HF (2019) Modeling the effects of health education and early therapy on tuberculosis transmission dynamics. Int J Nonlinear Sci Numer Simul 20:243–255
Xing Y, Song L, Sun GQ, Jin Z, Zhang J (2017) Assessing reappearance factors of H7N9 avian influenza in China. Appl Math Comput 309:192–204
Zhang F, Zhao XQ (2007) A periodic epidemic model in a patchy environment. J Math Anal Appl 325(1):496–516
Zhang YD, Huo HF, Xiang H (2019) Dynamics of tuberculosis with fast and slow progression and media coverage. Math Biosci Eng 16(3):1150–1170
Zhao XQ (2017) Dynamical systems in population biology, 2nd edn. Springer, Berlin
Zhao L, Zhang L, Huo HF (2019) Traveling wave solutions of a diffusive seir epidemic model with nonlinear incidence rate. Taiwan J Math 23(4):951–980